

Report 09/01/2020

P. Hacker

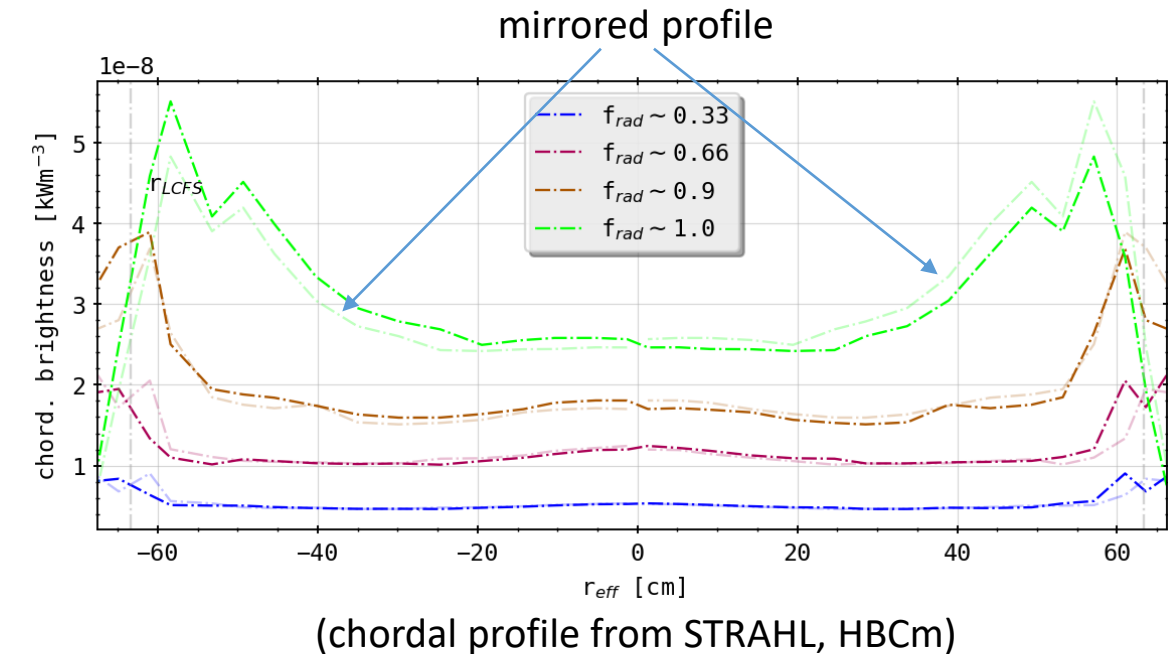
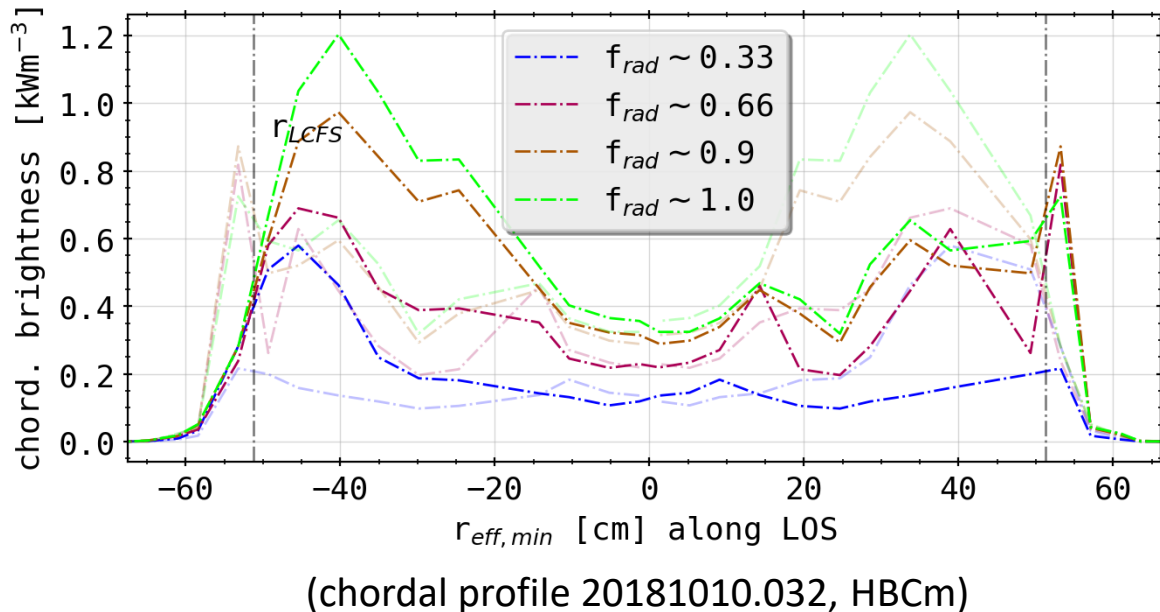


Previously: Geometry Sensitivity Study

- radiation feedback controlled discharge 20181010.032 shows transitions from no-stationary radiation states between 90%-100% radiation fraction
- with STRAHL simulate radiation profiles, given the electron temperature and density at distinct radiation fraction levels to investigate intrinsic (oxygen and carbon) impurity radiation
- STRAHL profiles show asymmetric chordal profiles after forward calculation with emissivity matrices, though being intrinsically symmetric

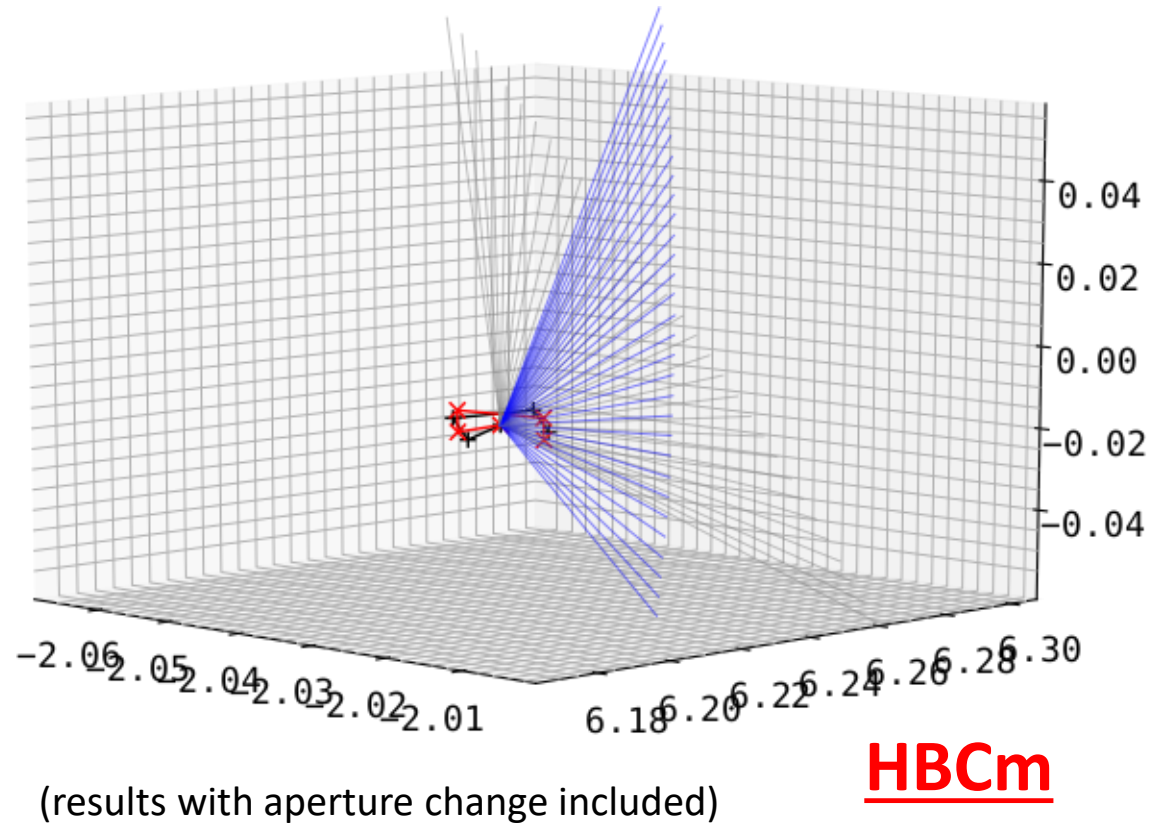
Previously: Geometry Sensitivity Study

- STRAHL profiles show asymmetric chordal profiles after forward calculation with emissivity matrices, though being intrinsically symmetric

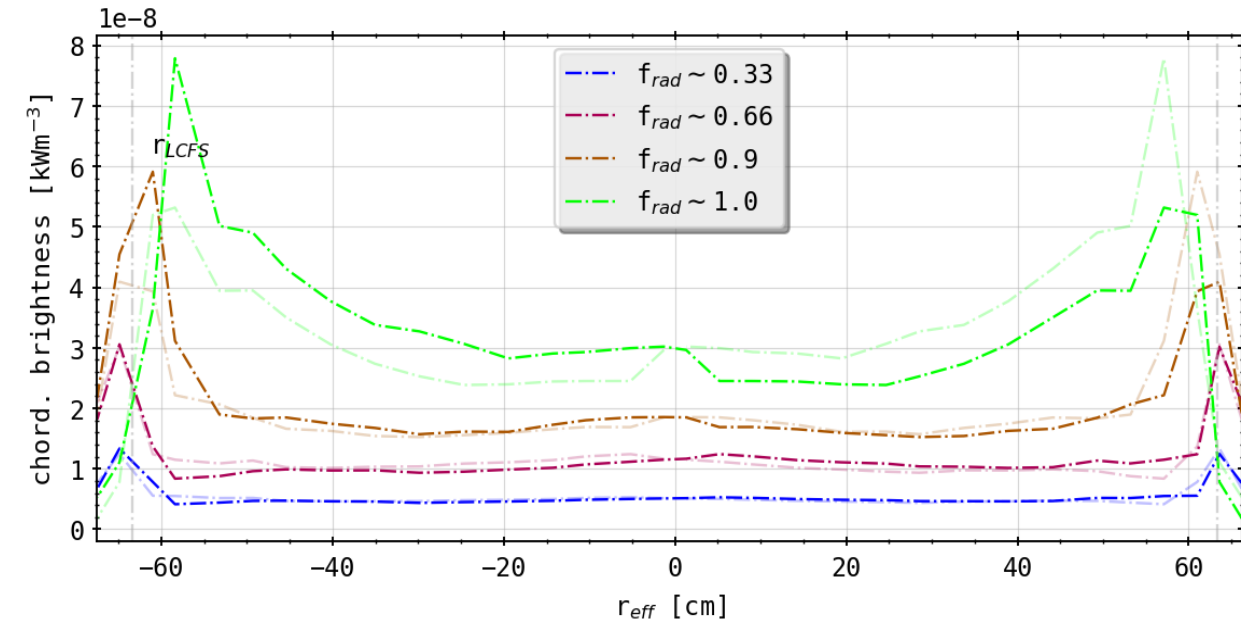


Results: Tilting the Detector Fan Up/Down

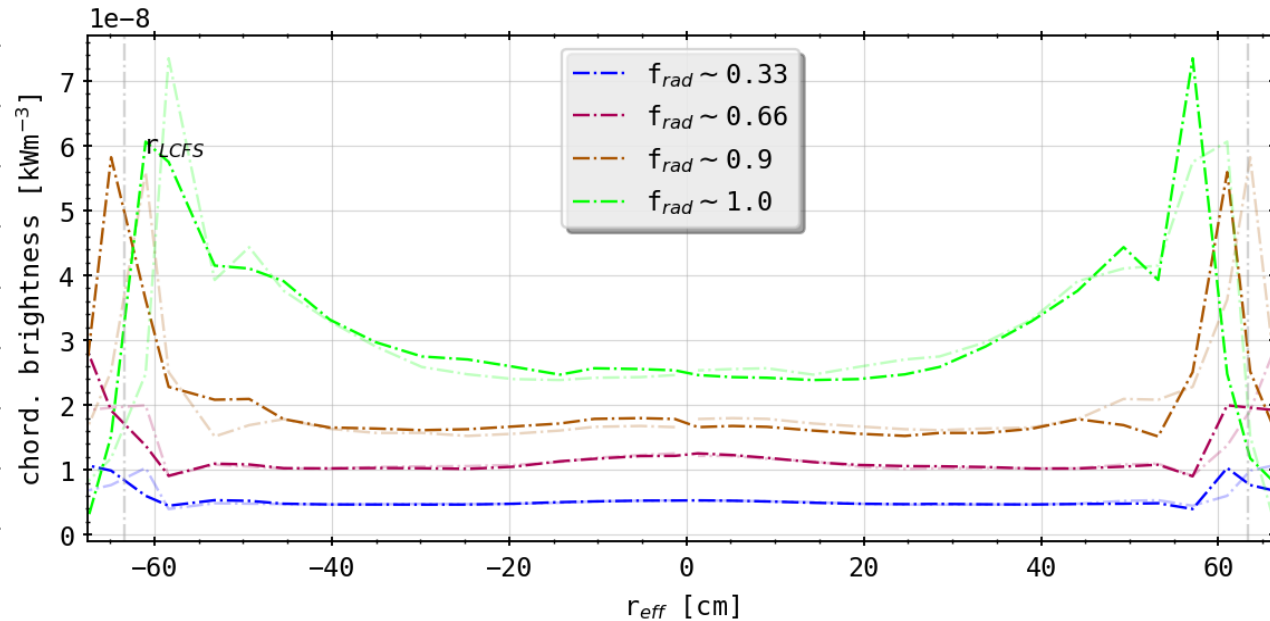
- deviance in STRAHL possibly results of intrinsic geometry
- ALSO: testing more effects that could change the intrinsic geometry, which can not be analysed
- e.g.: take symmetric arrays and tilt the entire fan including the aperture poloidally (grey to blue and black to red)



Results: Different Tilts from As-Built Geometry



(0.5° tilt (down))



(-0.5° tilt (up))

- asymmetry switchable/changed around
- alignment better now upside (tilt down!)
- radial movement as before and in original

First Summary

- geometry sensitivity study yields great insight on how the camera setup and errors effect forward calculations
- results show that variety and possibly a combination of measurement and intrinsic geometry errors are responsible for further asymmetries in results

Is the camera geometry adequate to resolve radial shifts in 2D from STRAHL?

→ need 2D tomography of radiation distribution

- benchmark Minimum Fischer Regularization method for 2D inversion using a variety of phantom radiation profiles with various distinct or mixed characteristics

Reference to Previous Results: 2D Projection

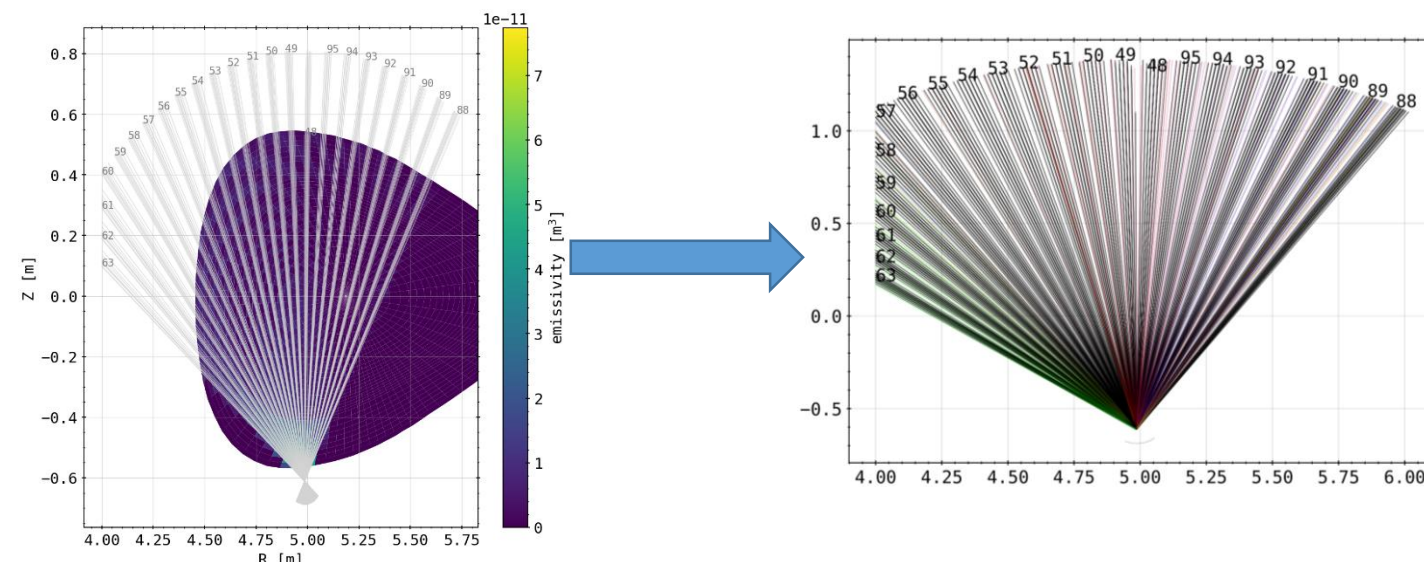
➤ previous investigations into surrogate profile benchmarks made based off an attempt to treat lines of sight and sensitivity matrices geometry in 2D, e.g. in the plane of the camera

however: errors made in treatment of (x,y,z) in plane of camera

➤ new approach: finding polar coordinates in camera plane and find fluxsurface geometry in each individual camera location

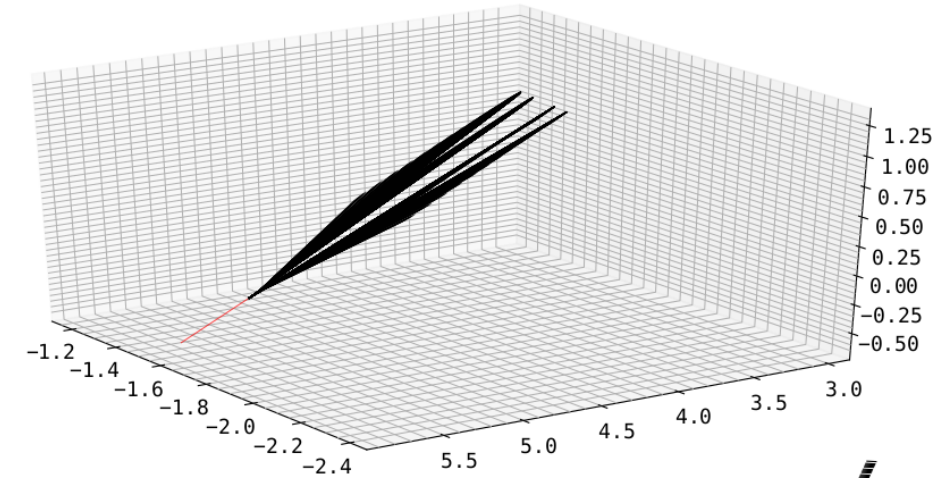
➤ cut of camera plane with vectors of fluxsurfaces in successive toroidal positions

(bad coverage of 64 individual center lines of sight from interpolated detector and pinhole geometry)

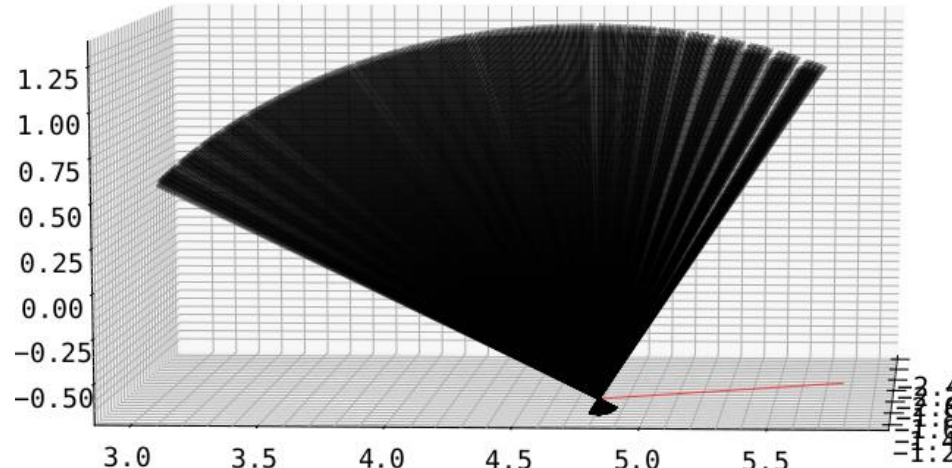


Reference to Previous Results: 2D Projection

- projection into '2D' by treating the LoS in respective camera plane through conversion into polar coordinates
- create **intersection vector** between camera and **xy-plane**, then find angle inbetween LoS and intersection
- take out-of-plane angle from camera and LoS into account for 'correct' line length measurement when looking at cell intersections

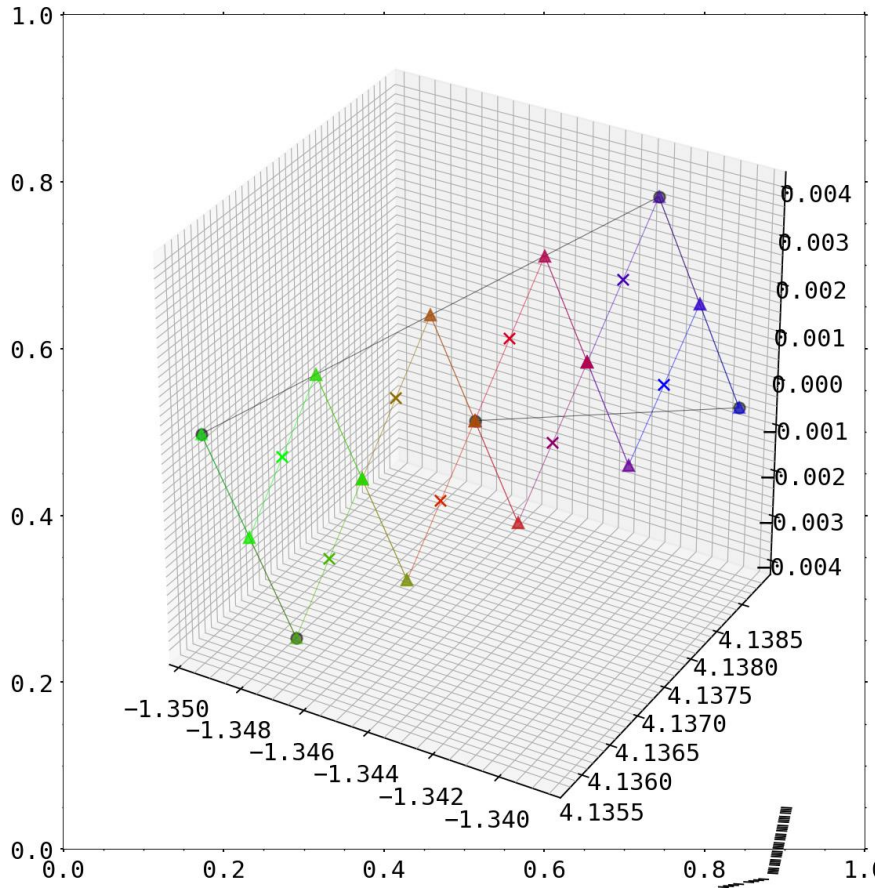
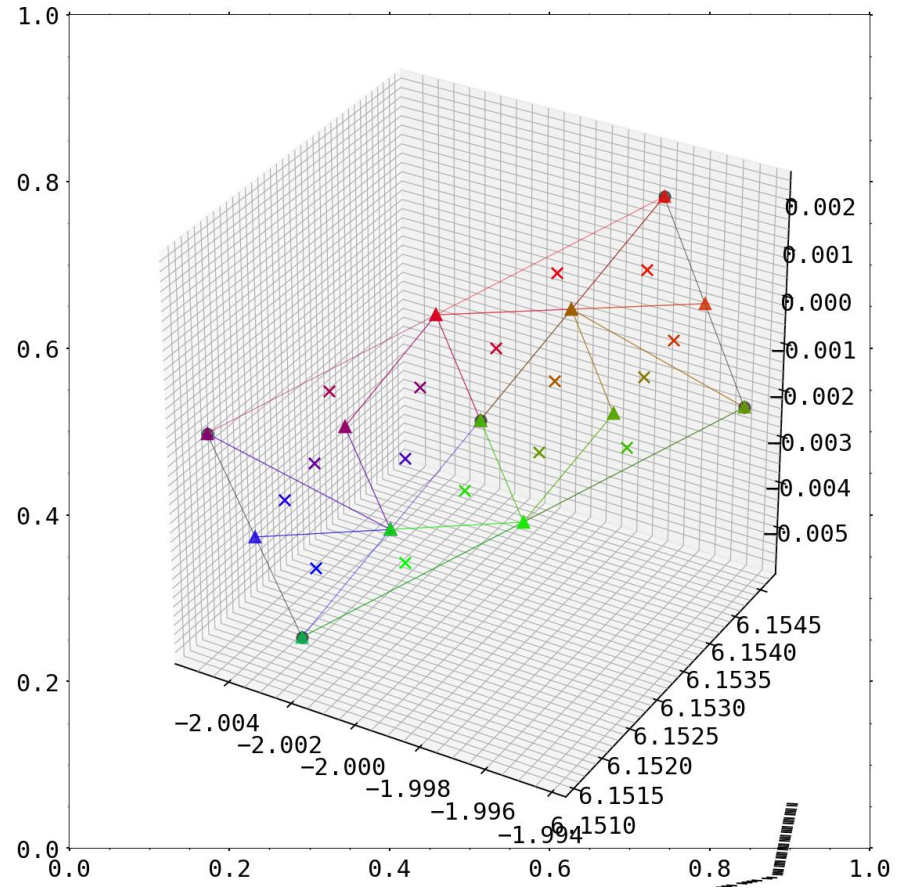


(VBCr with **intersection line to xy-plane**)



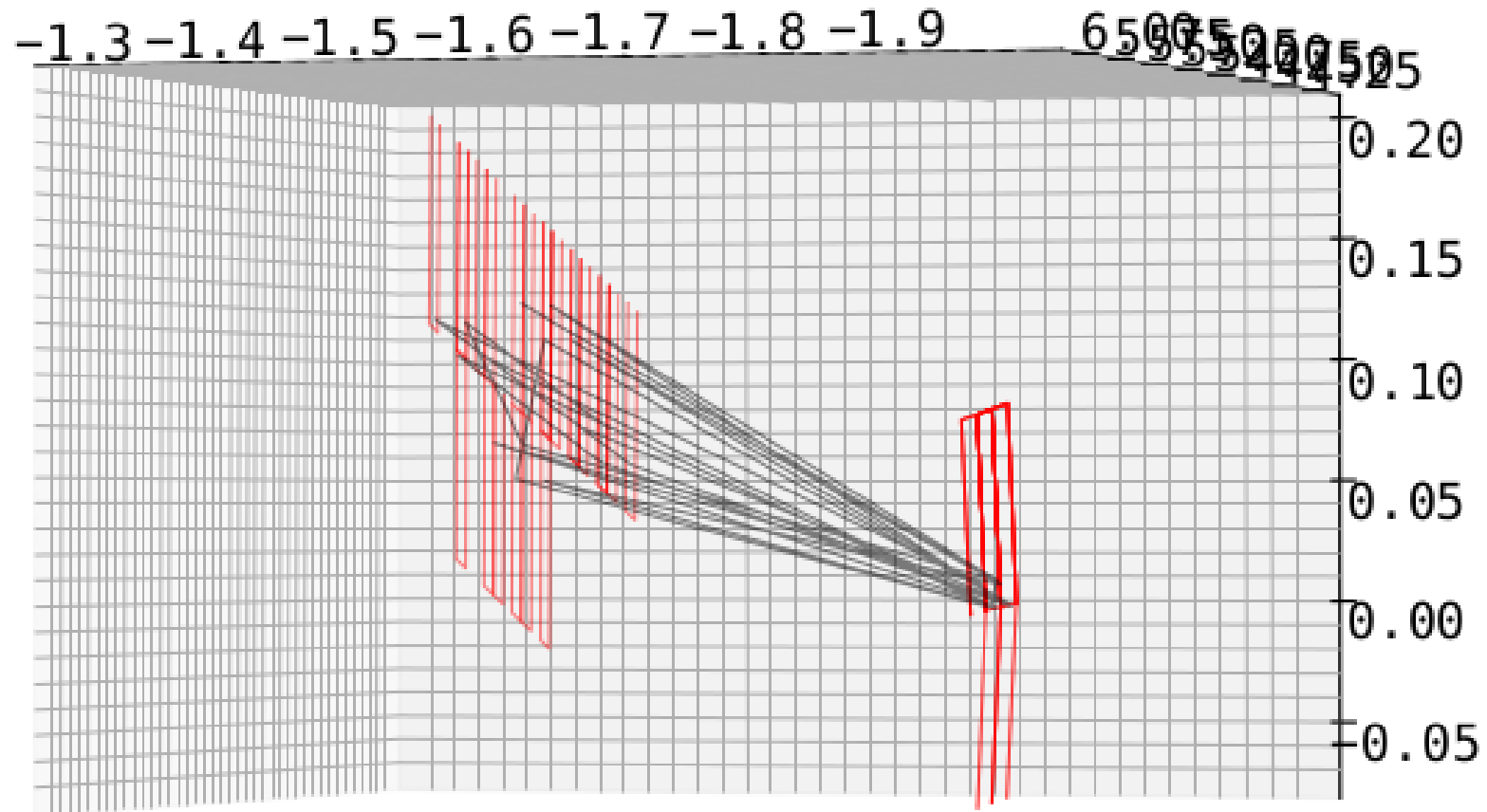
Reference to Previous Results: 2D Projection

- now also two modes of interpolation of detector/pinhole applied
triangulation
- **square**



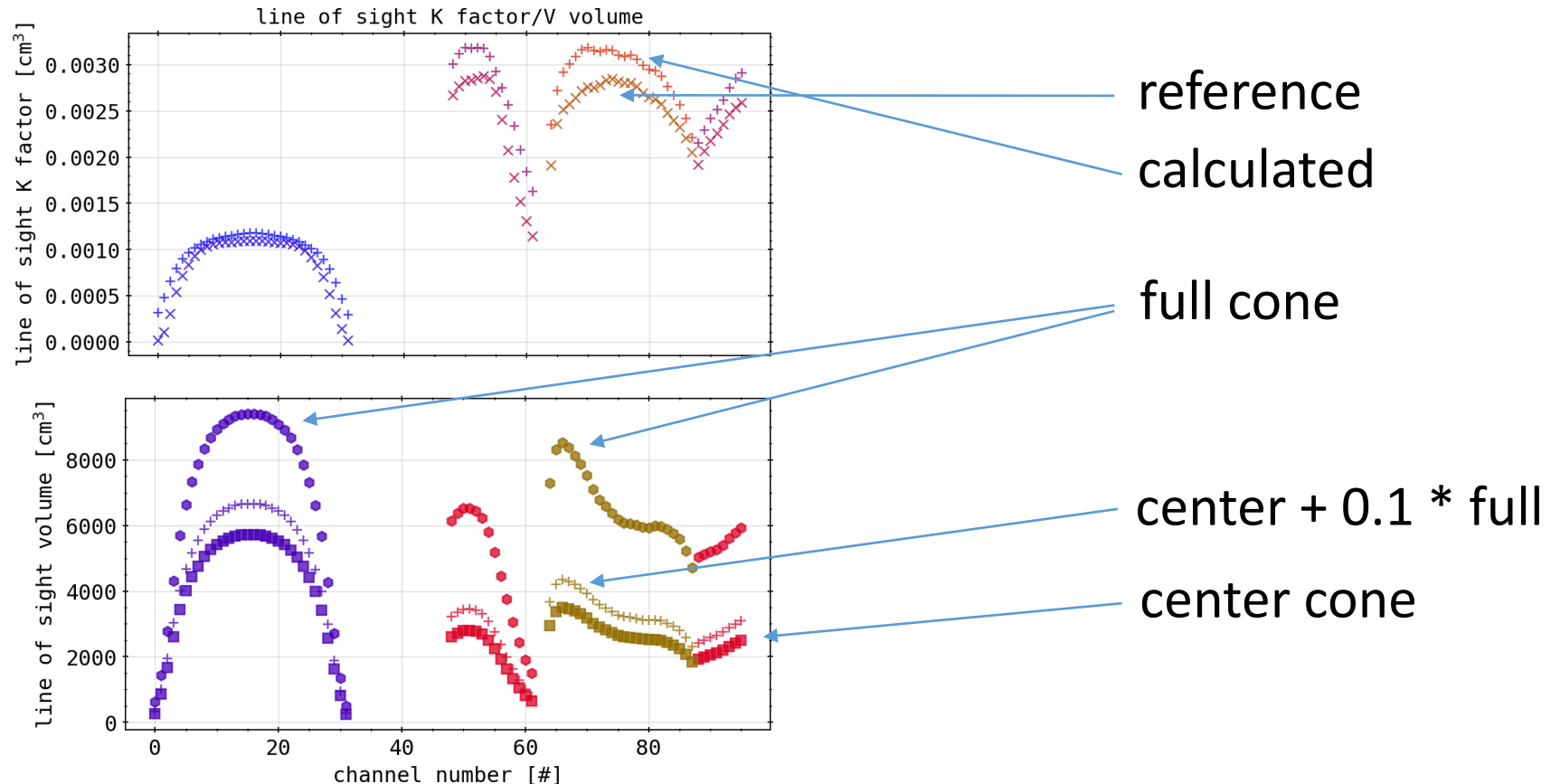
Reference to Previous Results: 2D Projection

- 3D line of sight cone projection through plasma shell with center and full volume
- 16 lines for the cone by projection of detector corners through aperture corners



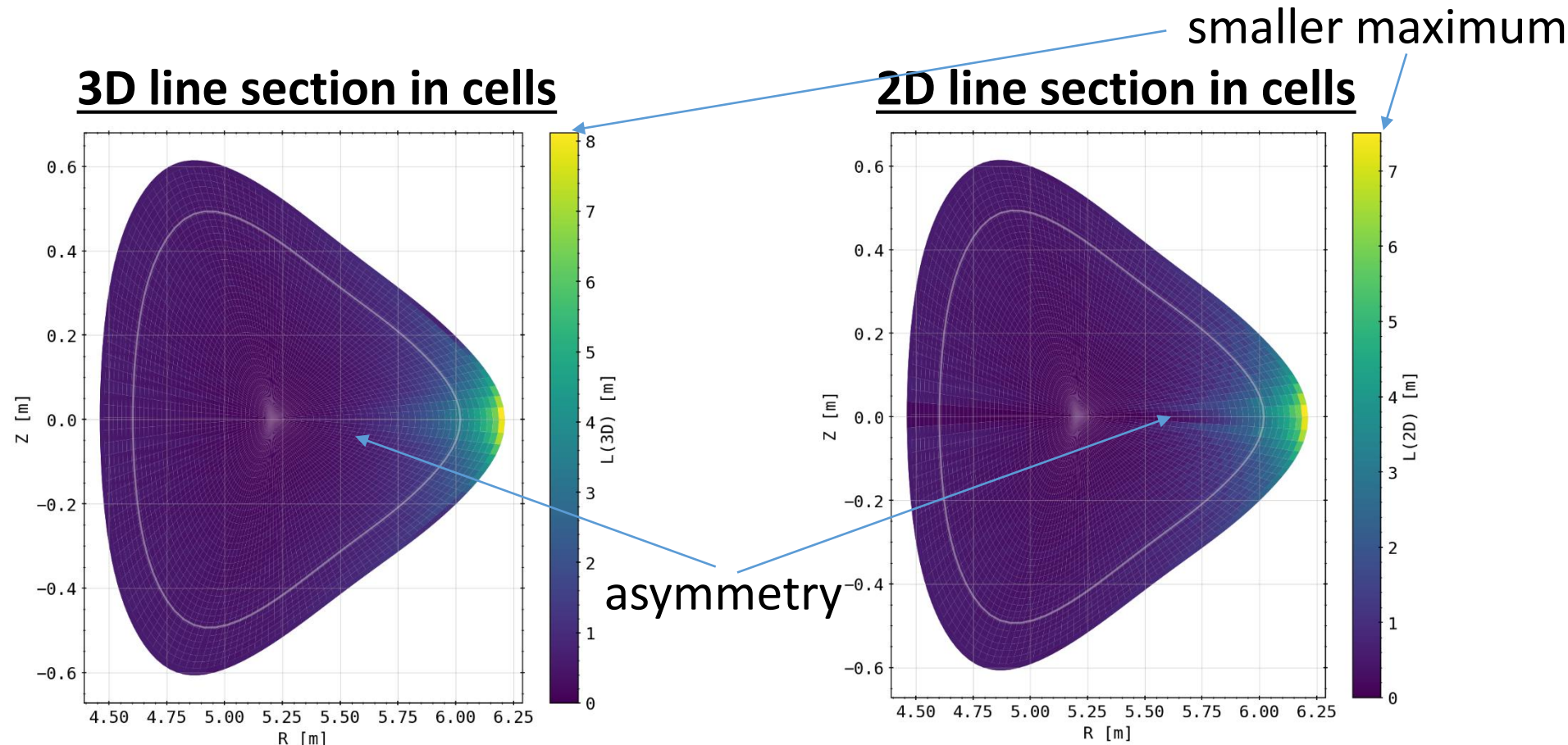
Reference to Previous Results: 2D Projection

- 3D line of sight cone projection through plasma shell with center and full volume
- 16 lines for the cone by projection of detector corners through aperture corners



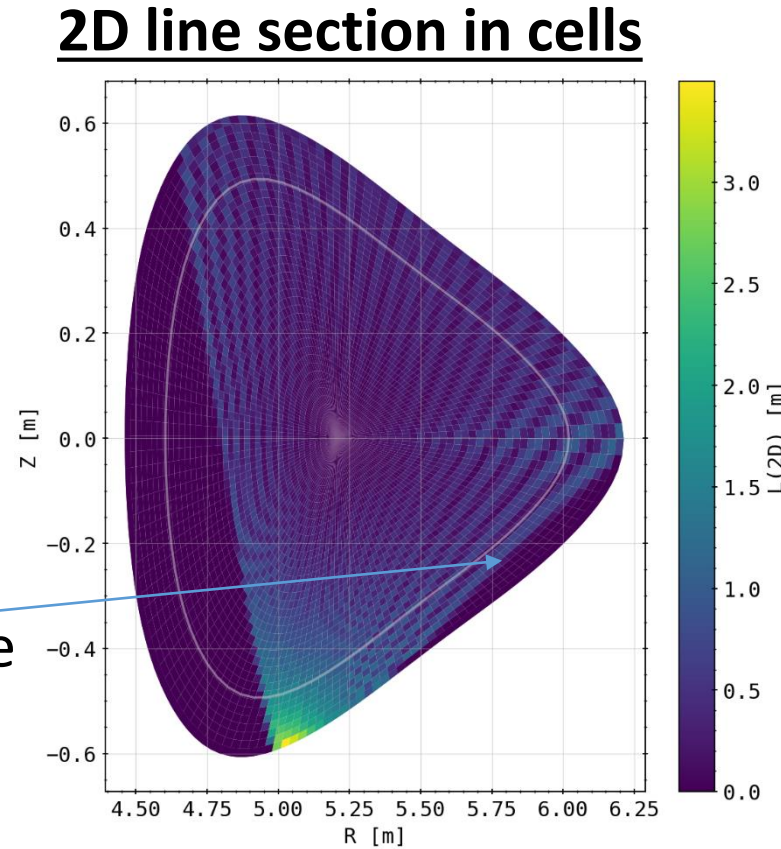
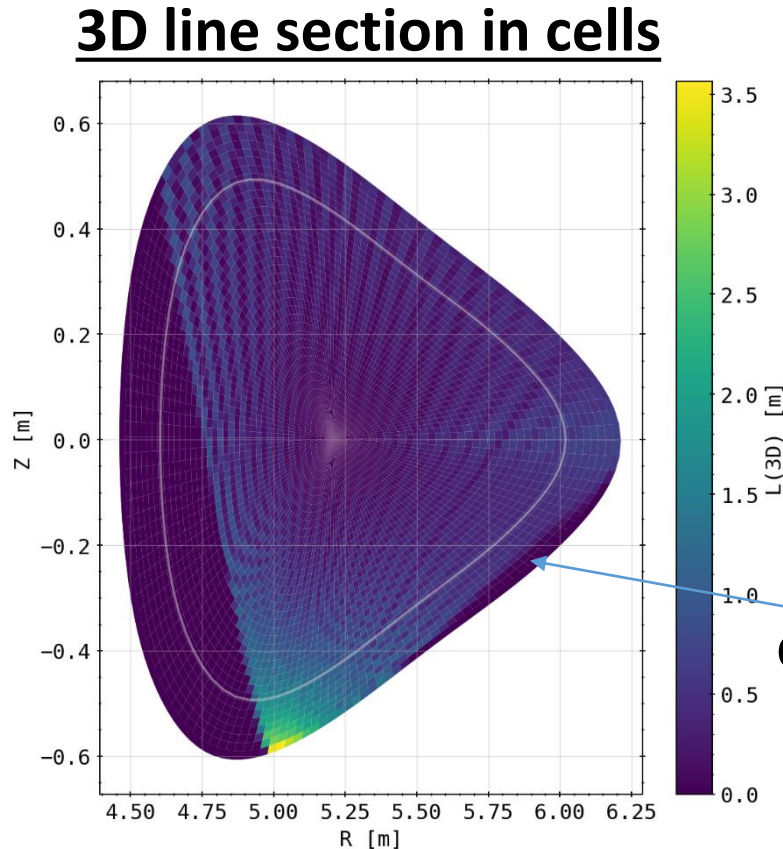
Reference to Previous Results: 2D Projection

- Applicable? If so, to what degree resemblance to real 3D geometry?
- 3D is result of condensing toroidal cells into plane of camera, 2D is directly only from plane with out-of-plane fix for length



Reference to Previous Results: 2D Projection

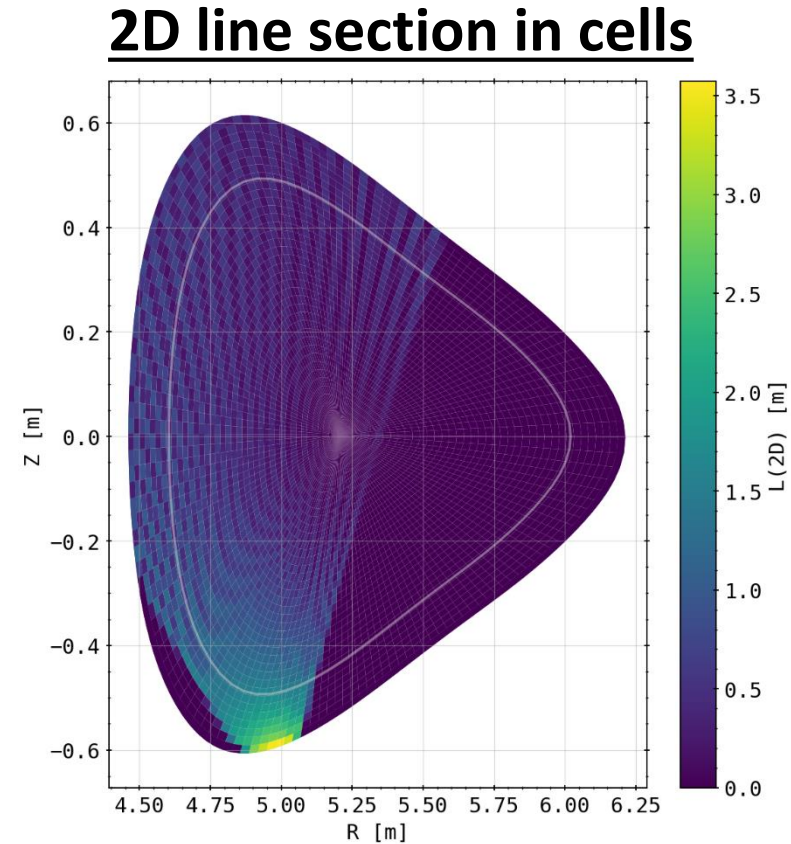
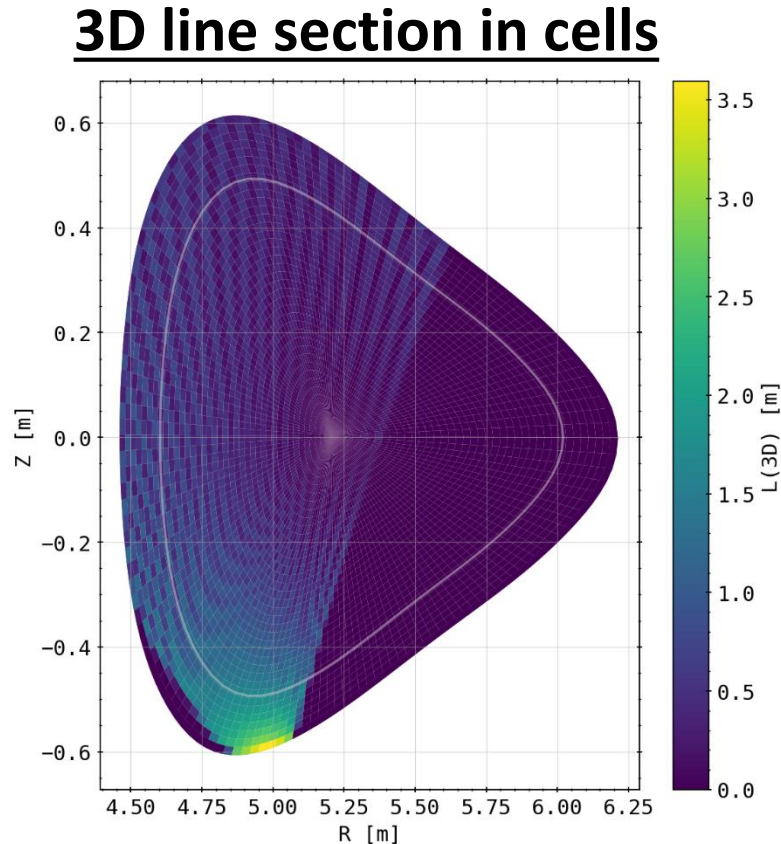
- Applicable? If so, to what degree resemblance to real 3D geometry?
- 3D is result of condensing toroidal cells into plane of camera, 2D is directly only from plane with out of plane fix for length



coverage

Reference to Previous Results: 2D Projection

- Applicable? If so, to what degree resemblance to real 3D geometry?
- 3D is result of condensing toroidal cells into plane of camera, 2D is directly only from plane with out of plane fix for length



Reference to Previous Results: 2D Projection

- Applicable? If so, to what degree resemblance to real 3D geometry?
- 3D is result of condensing toroidal cells into plane of camera, 2D is directly only from plane with out of plane fix for length
- **CONCLUSION:** 2D projection possible, does not entirely represent the full 3D setup of the Bolometry system at W7-X
- for a more planar line of sight cone projection might be applicable, has to be treated in camera plane
- biggest deviance from coverage of pixel areas (or not) which can not be accounted for in 2D
- **next: results from 3D calculations**

Phantom Test: Poloidal Gradient Factor

$$D_{\text{iaR}} = 1^{n_x \times n_\varphi}$$

$$D_{\text{iaR}} = 1_{\text{next line}}^{n_x \times n_\varphi}$$

$$D_{\text{iaL}} = 1_{\text{previous line}}^{n_x \times n_\varphi}$$

$$D_{\text{iaU}} = 1_{\text{next pixel}}^{n_x \times n_\varphi}$$

$$D_{\text{iaD}} = 1_{\text{previous pixel}}^{n_x \times n_\varphi}$$

K : smoothness/gradient factor

$$\mathrm{d}r = R_1 - R_0$$

$$\mathrm{d}\varphi_{\text{FS}} = K \cdot \mathrm{d}r_{\text{FS}} \cdot (\varphi_1 - \varphi_0)$$

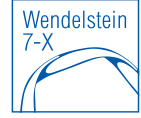
r gradient: $B_r = D_{\text{iaR}} - D_{\text{iaM}}$ $B_{\varphi, \text{FS}} = \frac{B_\varphi}{\mathrm{d}\varphi_{\text{FS}}}$

phi gradient: $B_\varphi = D_{\text{iaU}} - D_{\text{iaM}}$ $B'_r = \frac{B_r}{\mathrm{d}r}$

$$A_r = 1^{n_r \times n_\varphi} \cdot B_r , \quad A_\varphi = 1^{n_r \times n_\varphi} \cdot B_{\varphi, \text{FS}}$$

$$H = B_r^\top \cdot A_r + B_\varphi^\top \cdot A_\varphi$$

Phantom Test: Poloidal Gradient Factor



$$A_r = 1^{n_r \times n_\varphi} \cdot B_r , \quad A_\varphi = 1^{n_r \times n_\varphi} \cdot B_{\varphi, \text{FS}}$$

$$H = B_r^\top \cdot A_r + B_\varphi^\top \cdot A_\varphi$$

$$\sigma = \frac{1}{dU_f} \cdot 1^{n_r \times n_\varphi}$$

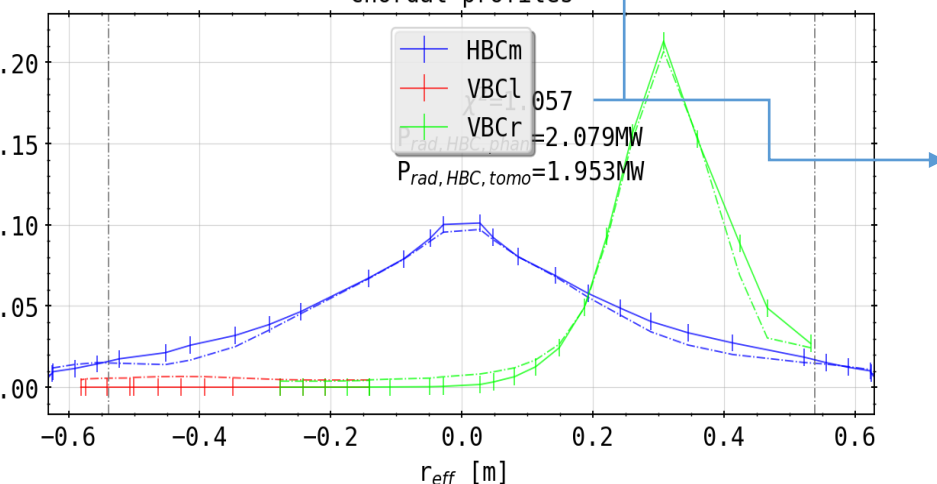
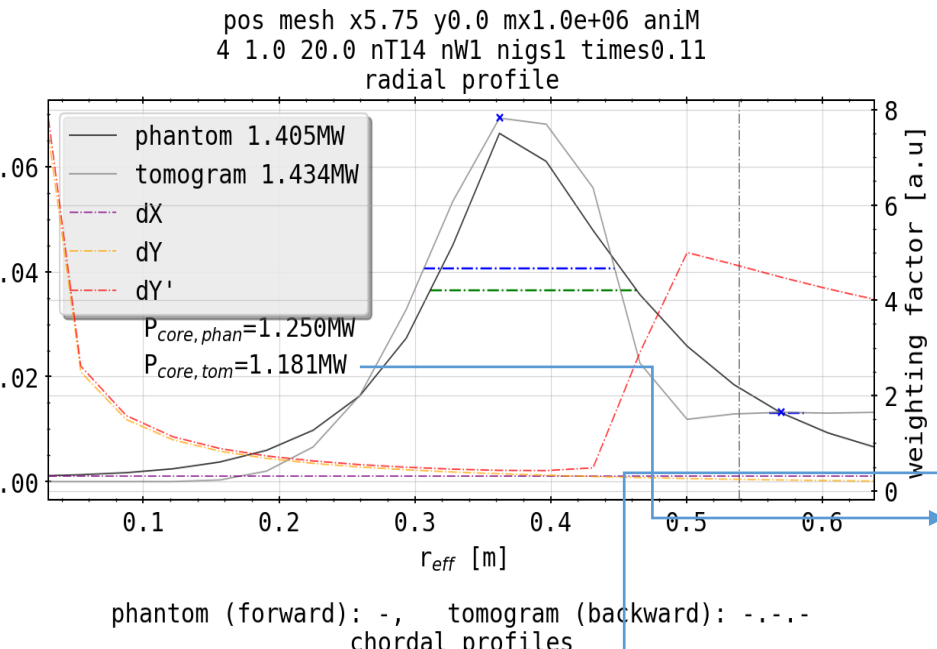
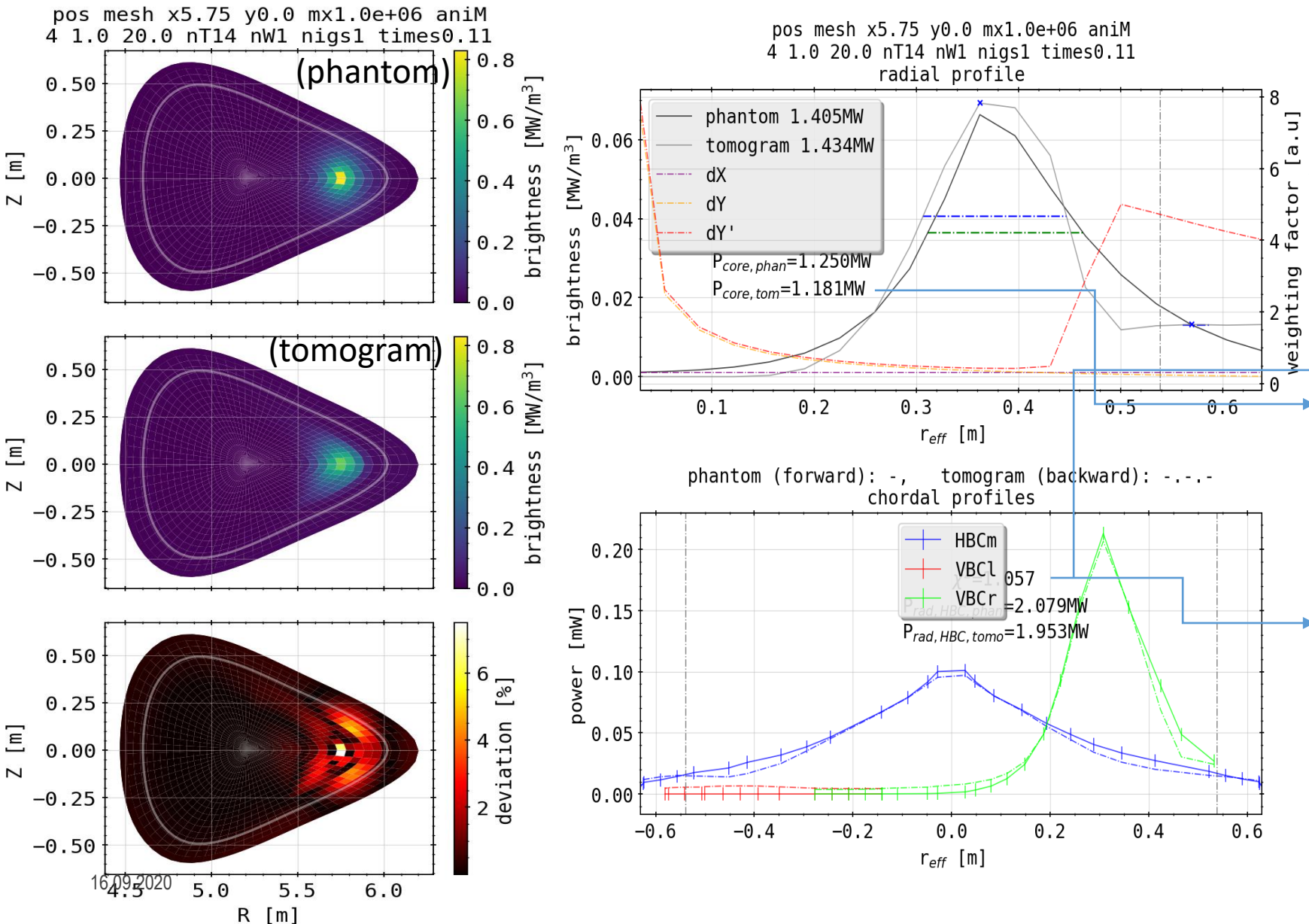
$$T_S = \sigma \cdot T_{\text{geom}}$$

$$T_T = T_S^\top \cdot T_S \propto \frac{1}{(dU_f)^2}$$

$$A = (T_T + \lambda \cdot H)$$

$$R_{\text{phantom}} = \text{least squares} (A, T_S^\top \cdot f)$$

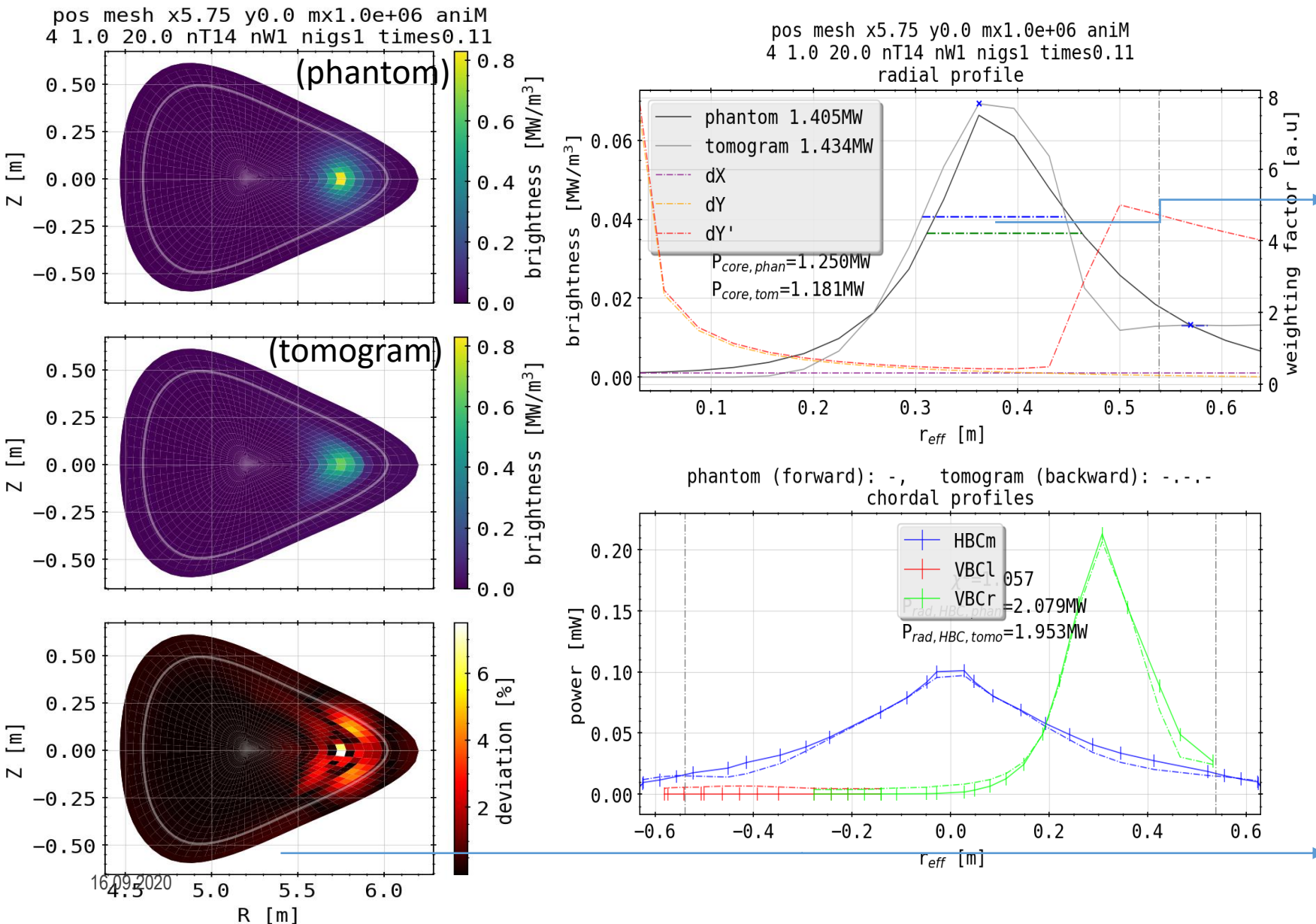
Phantom Test: Single Spot Off-Center



general remarks

- radiation power calculated *as usual* like in experiments
- total & core power estimated by hollow cylinders of fluxsurfaces from radial profile (unit errors, fix needed)
- X² measurement for congruence of forward and backward profiles (1.0 optimum)

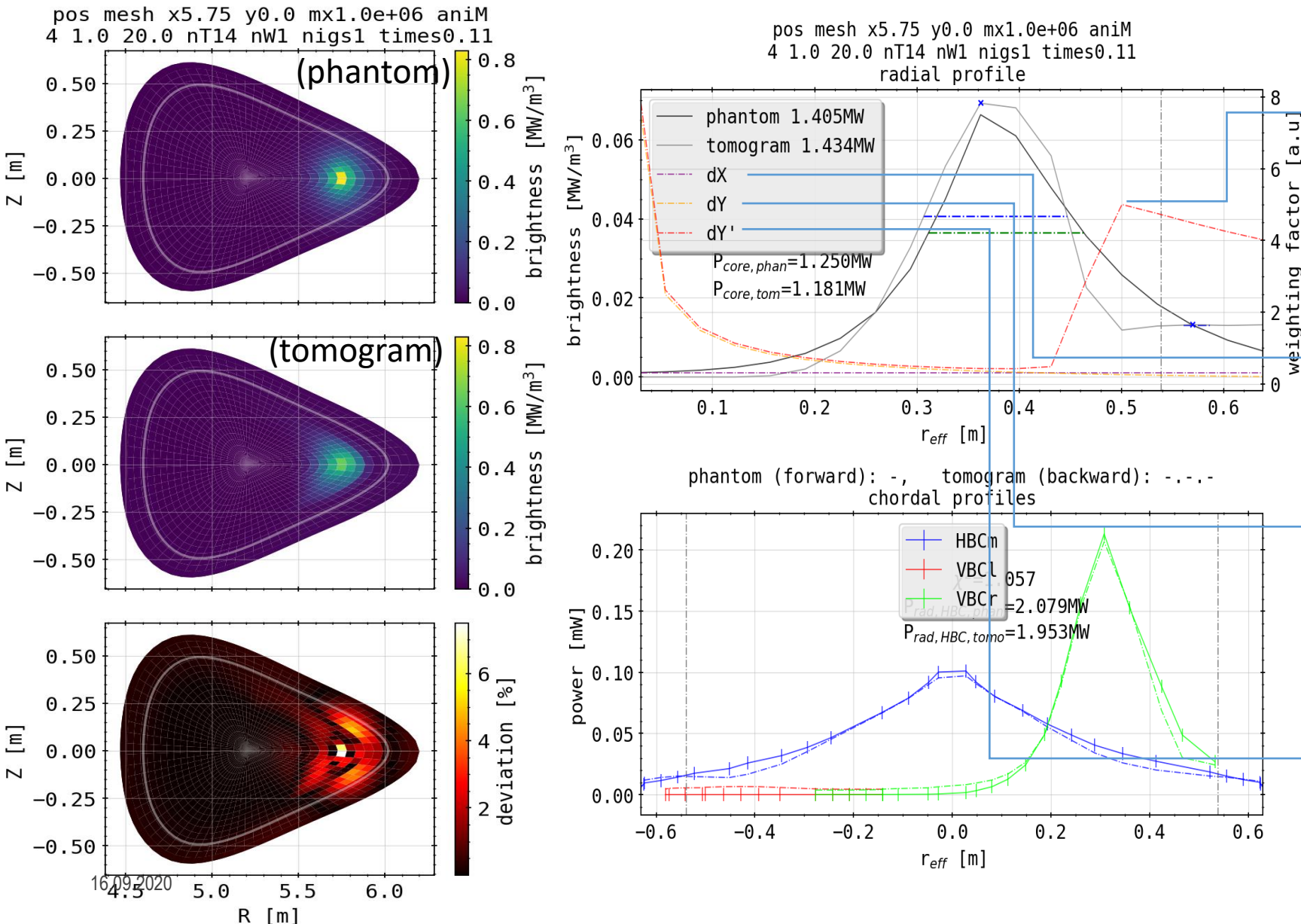
Phantom Test: Single Spot Off-Center



general remarks

- radial profile peak localization and width of distribution
- χ^2 quality does not necessarily equal best tomogram, hence the need for 2D relative deviation as measure to find best fit
- deviation percentage relative to area of cell & domain

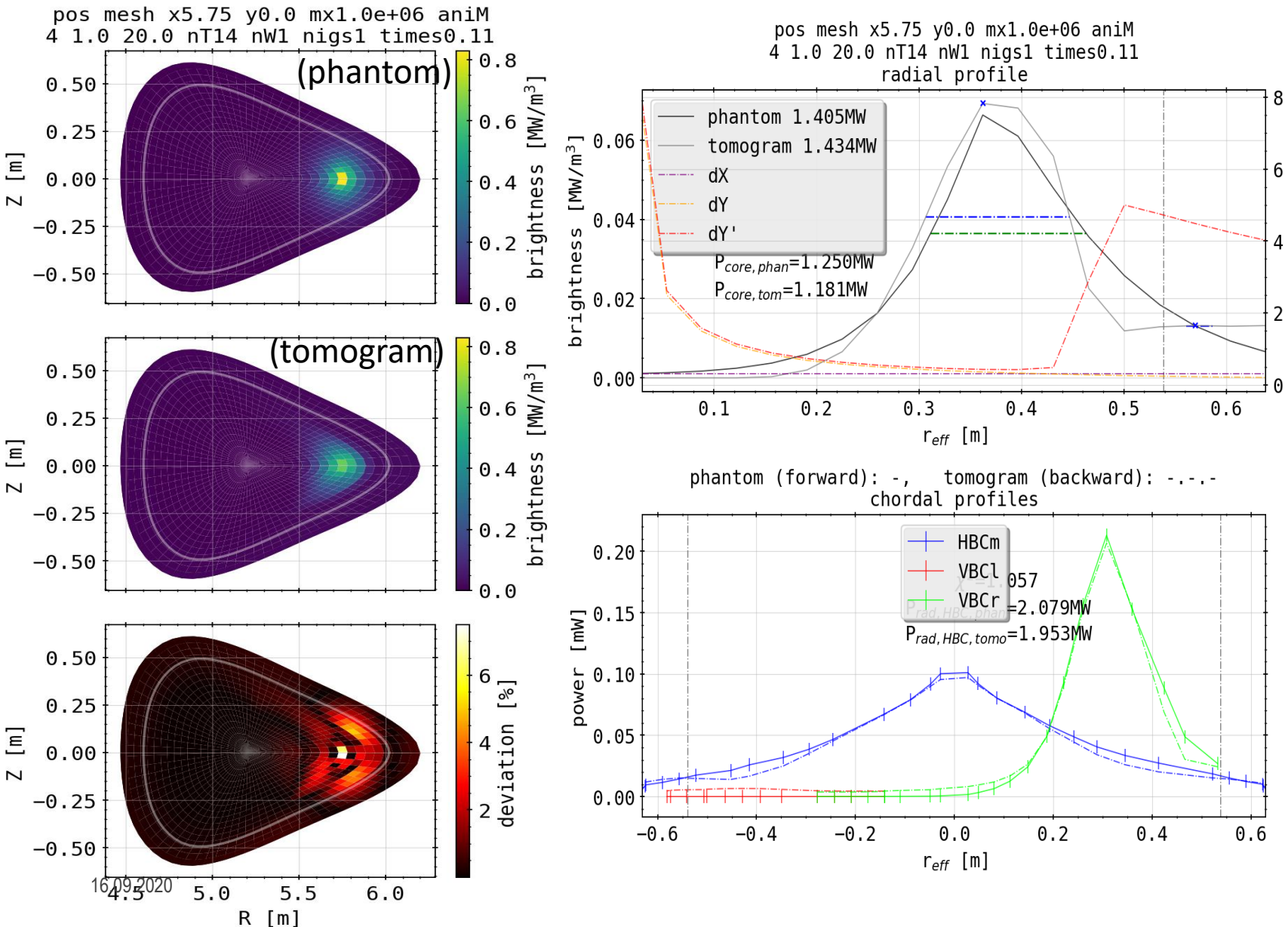
Phantom Test: Single Spot Off-Center



general remarks

- smoothing along fluxsurfaces, according to weighting of derivatives
- dX: gradient in radial direction; does not change across inversion domain
- dY: poloidal gradient length scale; high at center/inside confinement area, small outside
- dY': weighted poloidal gradient with input profile

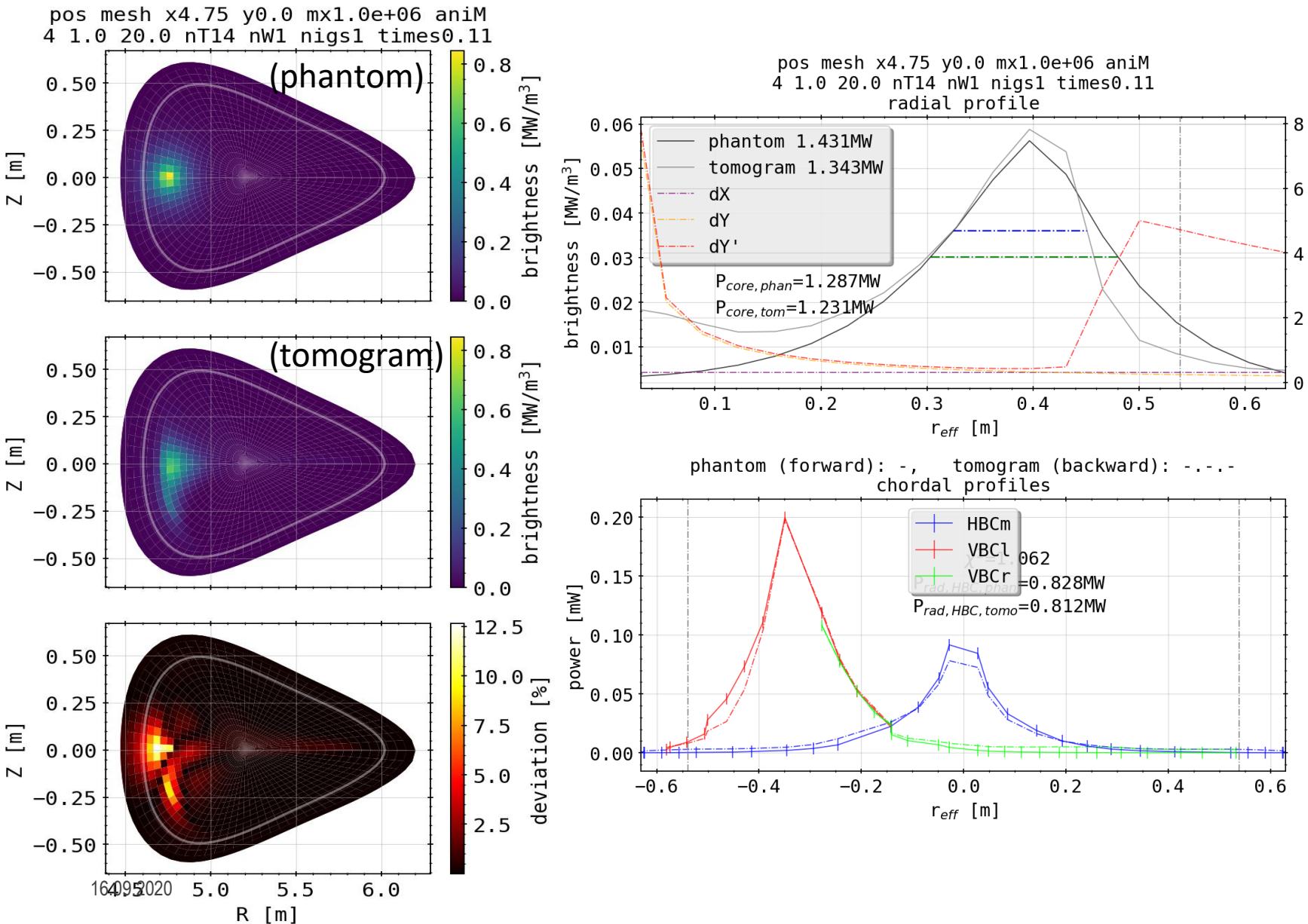
Phantom Test: Single Spot Off-Center



on the surrogate

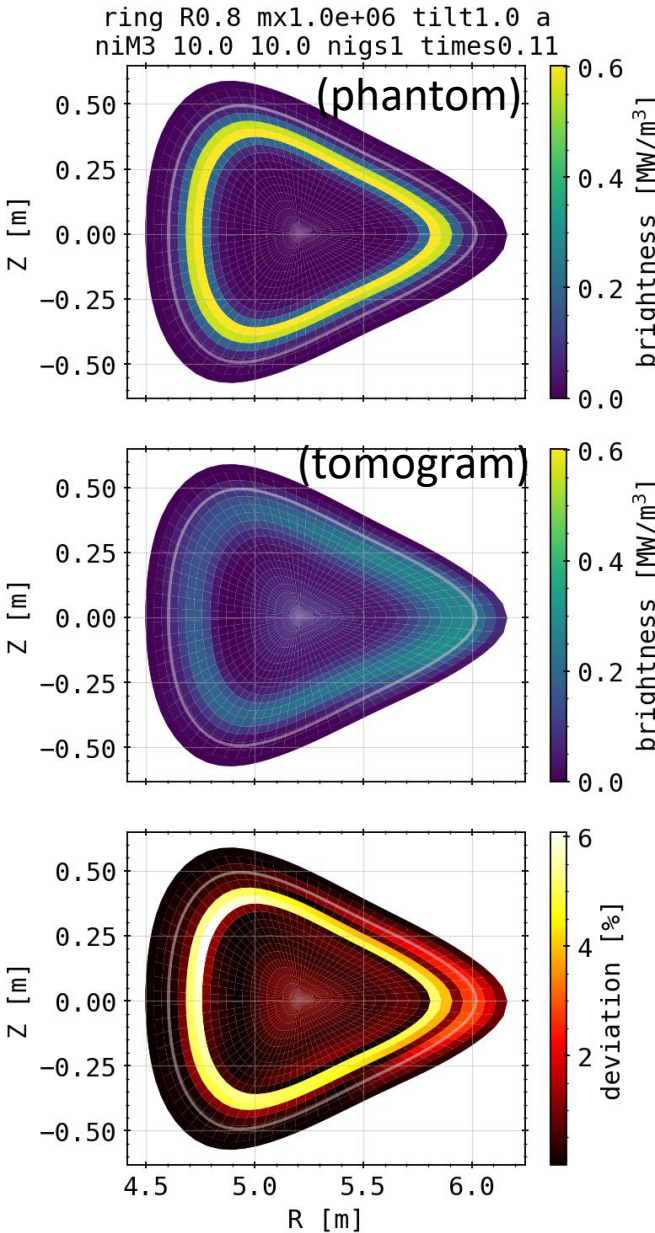
- very unrealistic, hard to reconstruct surrogate
- radial positioning good if K profile dialed
- poloidal smoothing at minimum, smaller values yield artifacts or redistribution to different areas of domain
- calculated powers match

Phantom Test: Single Spot Off-Center

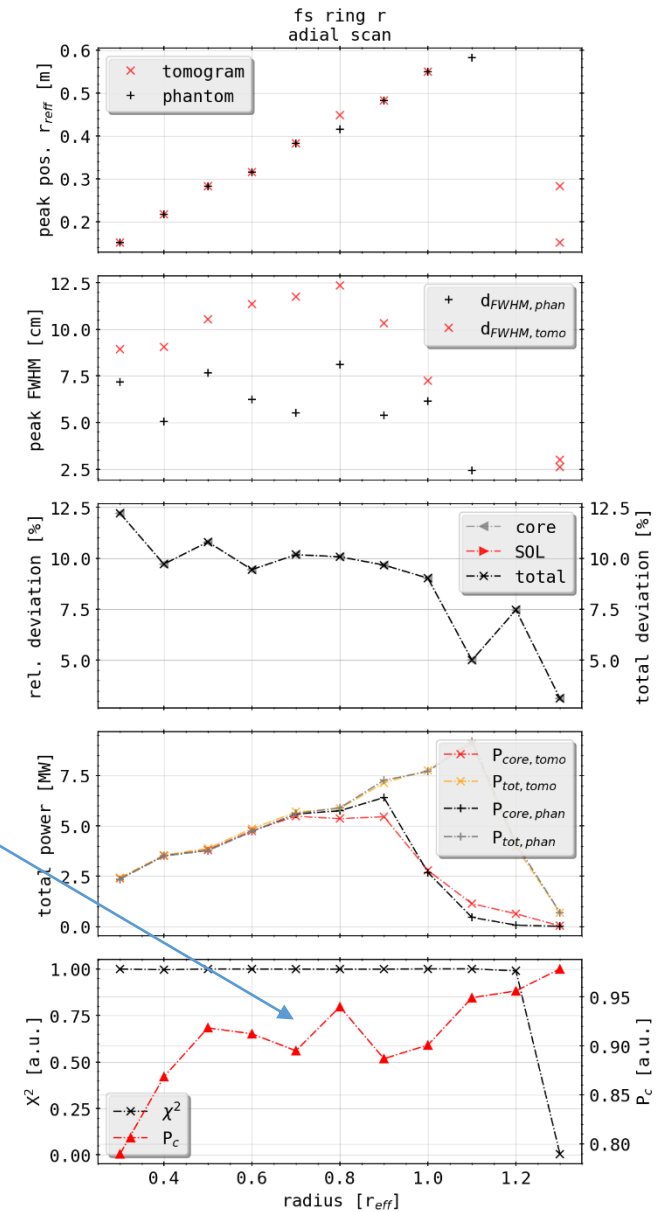


- radial position equally accurate, reflected as well in radial profile
- poloidal smoothing worse, suspect to tangential lines of sight from vertical camera arrays
- extrapolated radiation power loss from chordal profiles ~30-40% lower
- absorption of HBCm smaller and 2x the 2D error

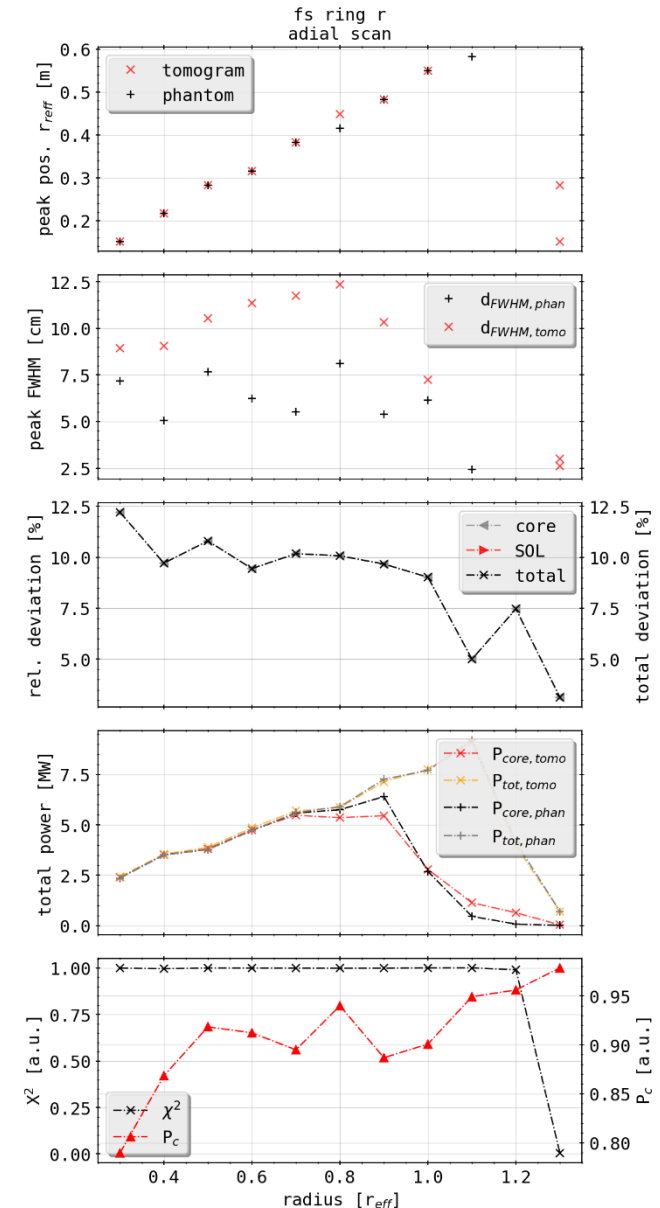
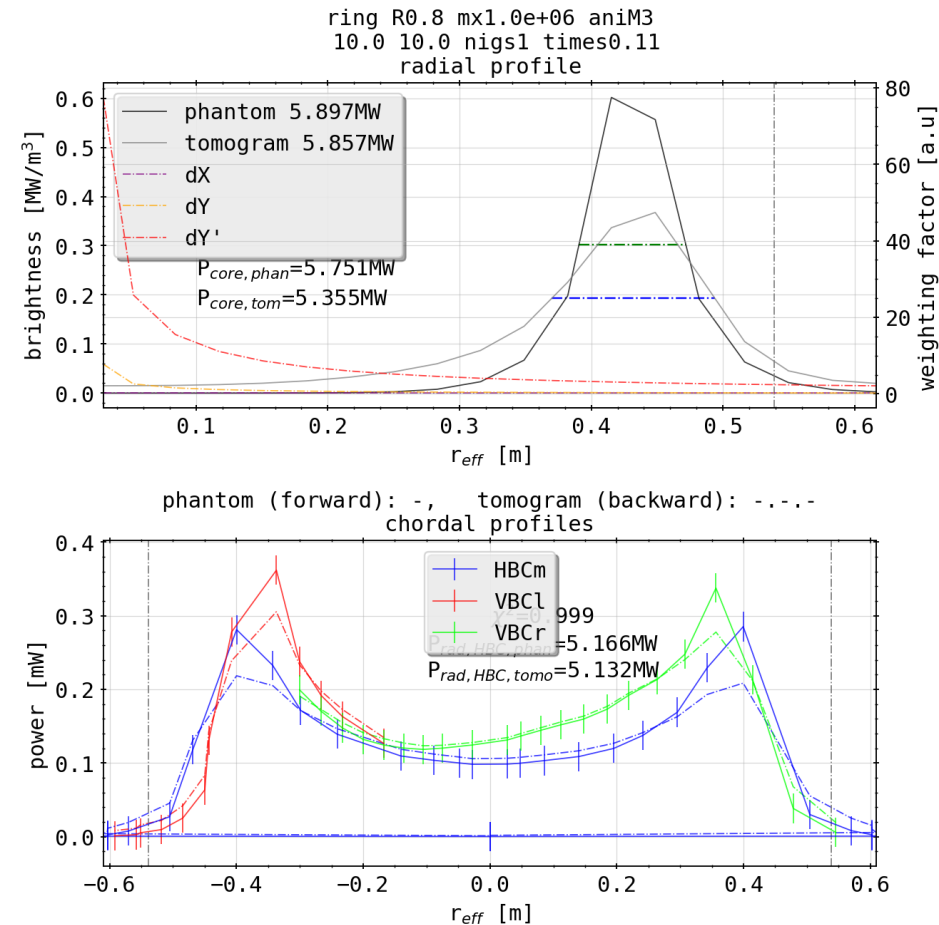
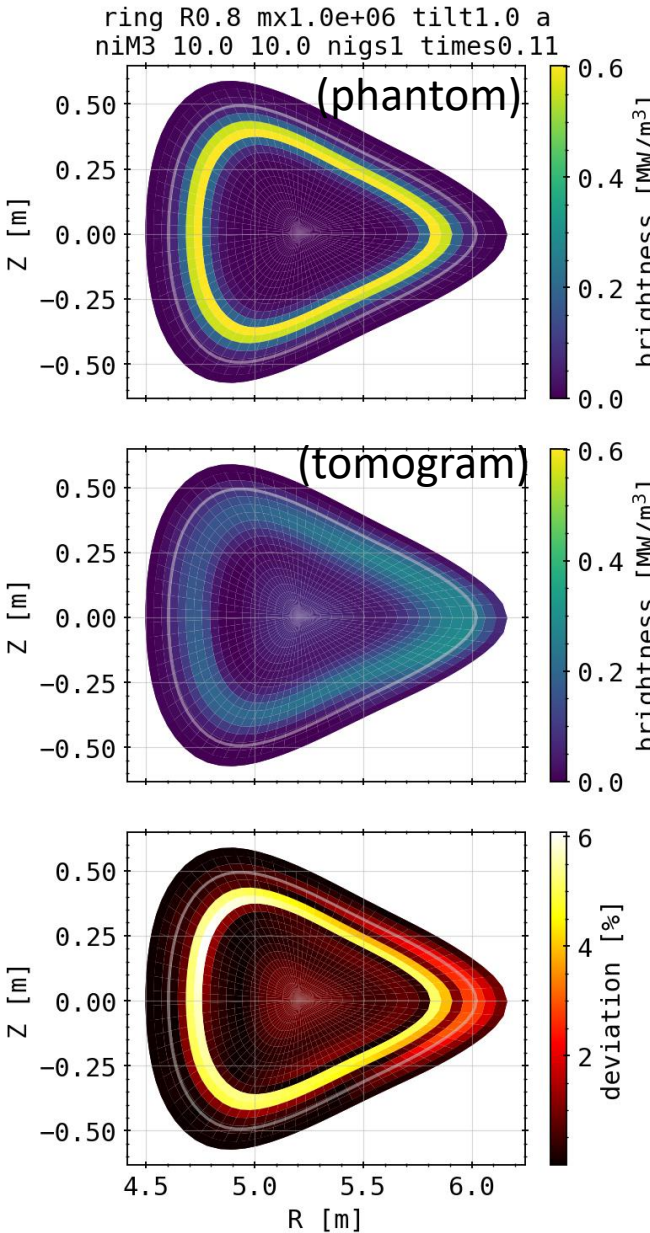
Phantom Test: Single Bright Ring



- scanning over the radial position of the ring, e.g. in units of the minor radius
- radial peak location matched accurately, although peak/profile shape distorted in radial direction
- χ^2 fits perfectly until degeneration when only edge of domain is bright
- incorporated *Pearson coefficient* measures cross correlation between 2D profiles of phantom and tomogram, i.e. better number for accuracy
- χ^2 optimum is not matched with neither Pearson coeff. or 2D deviance

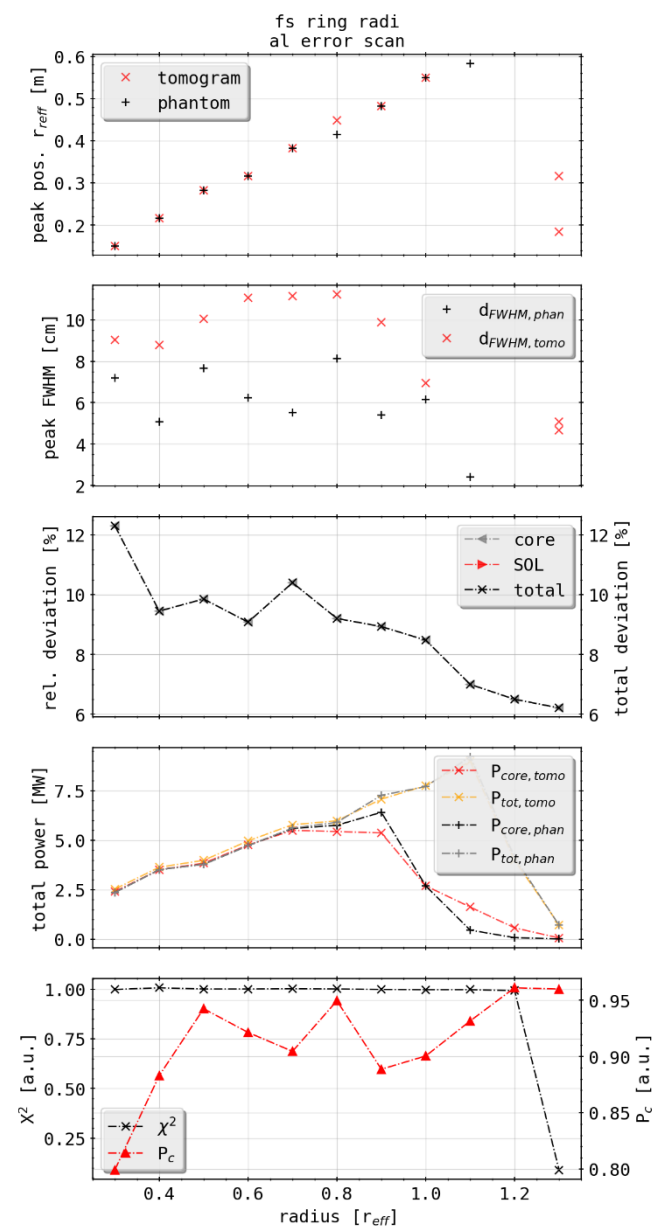
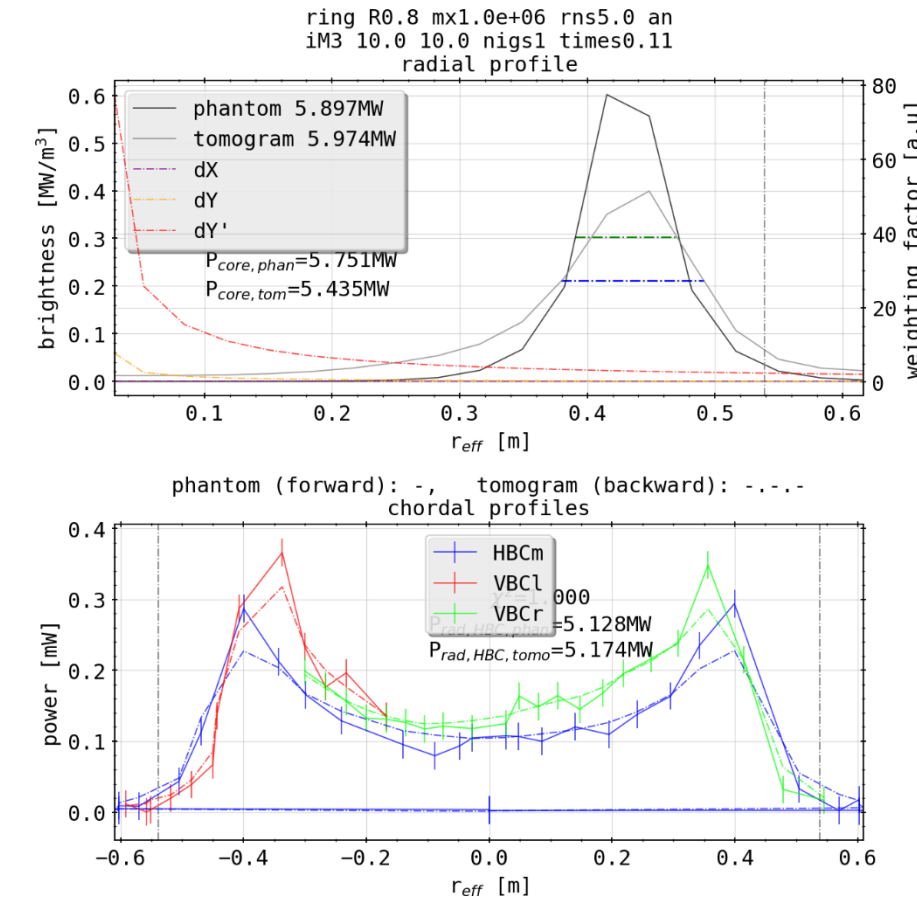
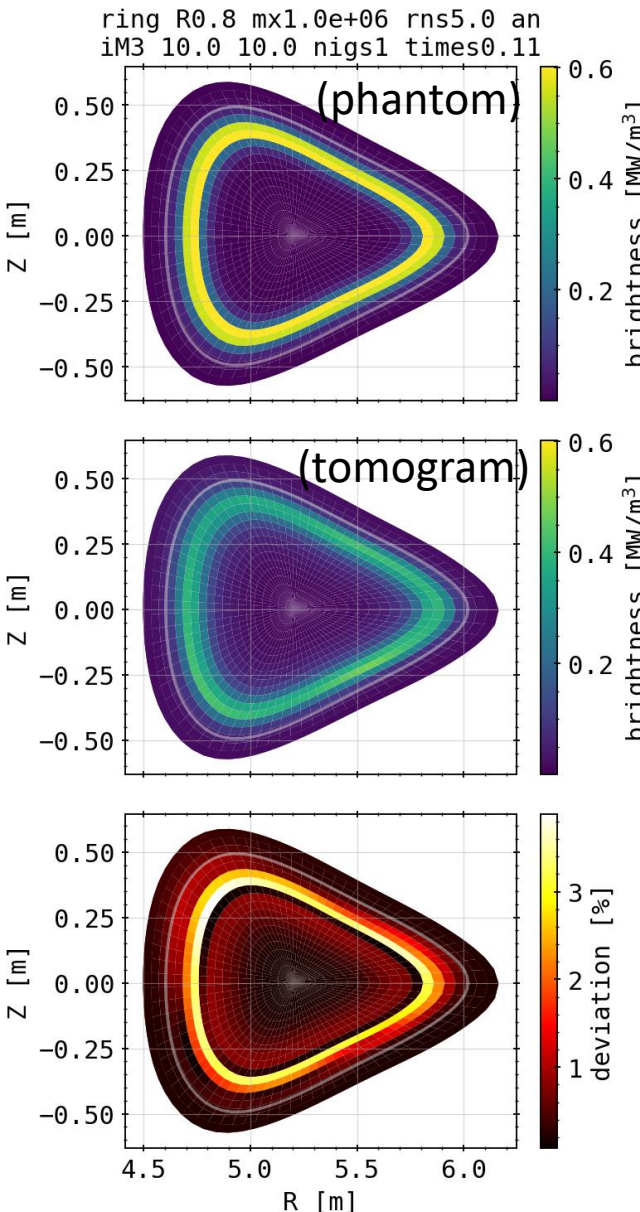


Phantom Test: Single Bright Ring



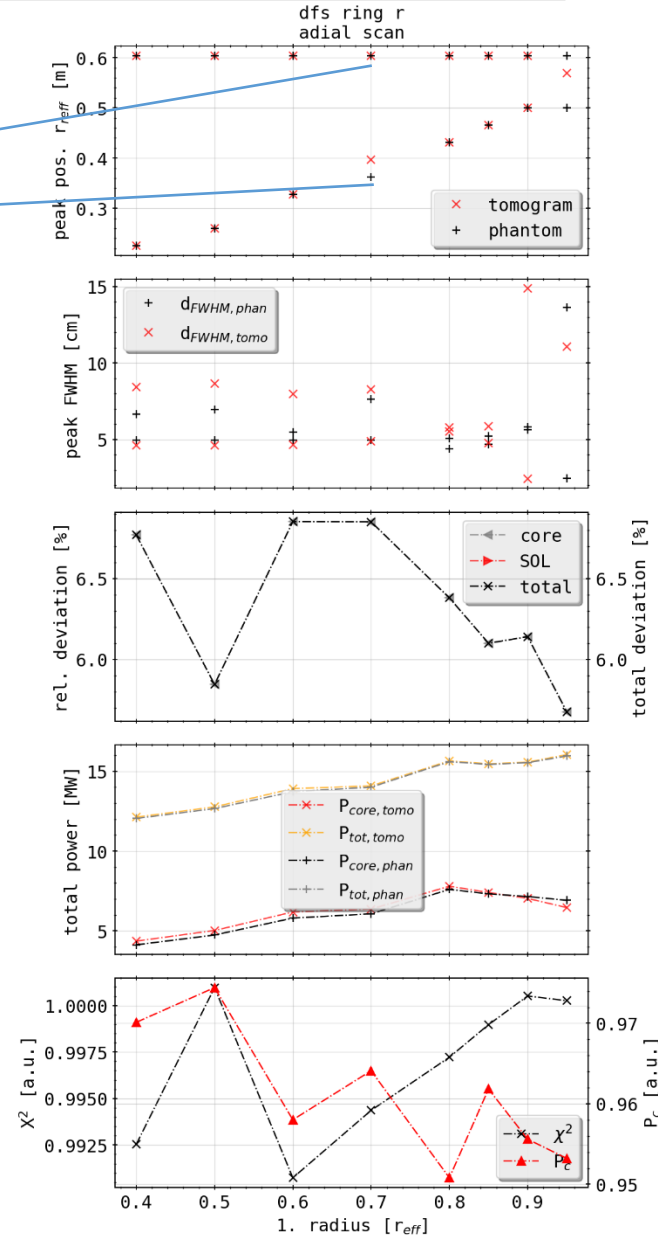
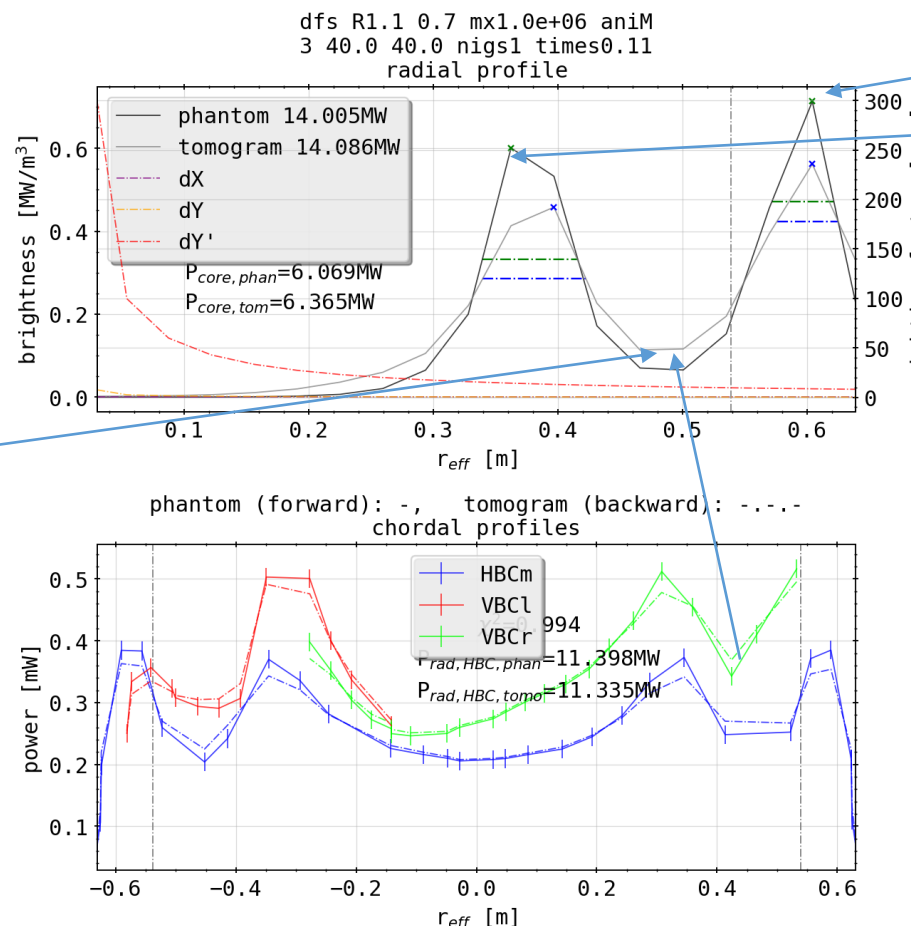
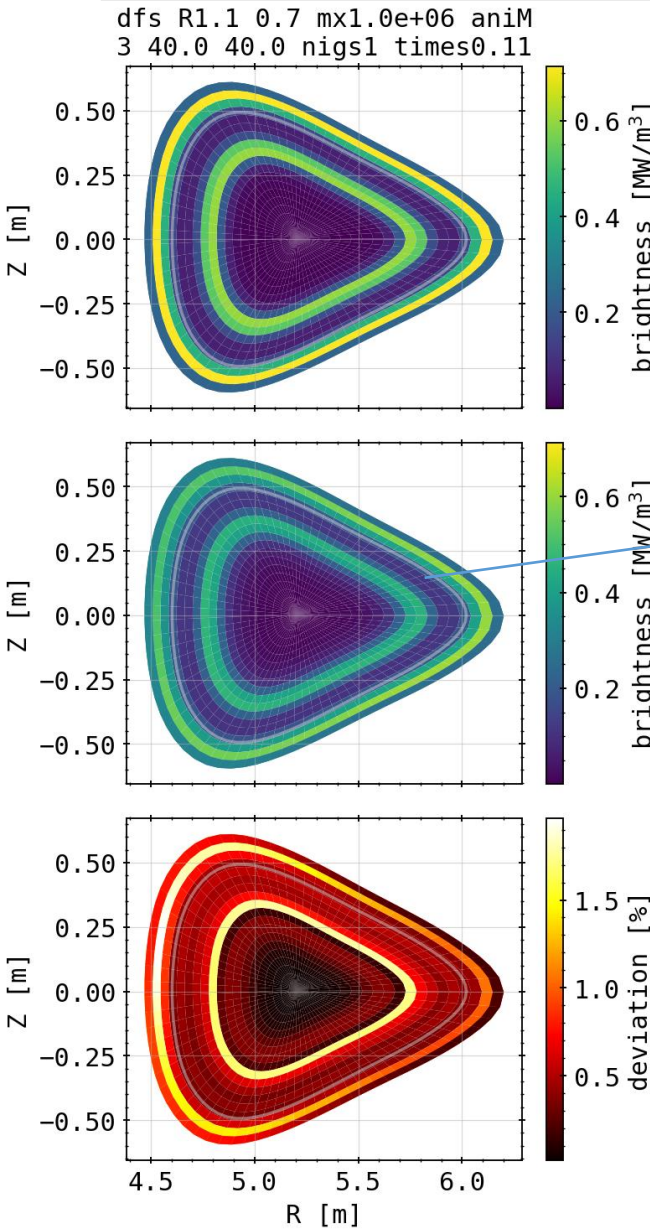
- good radial match, broader distribution and lower intensity
- overall integrated power however equal

Phantom Test: Single Bright Ring w. 5% error



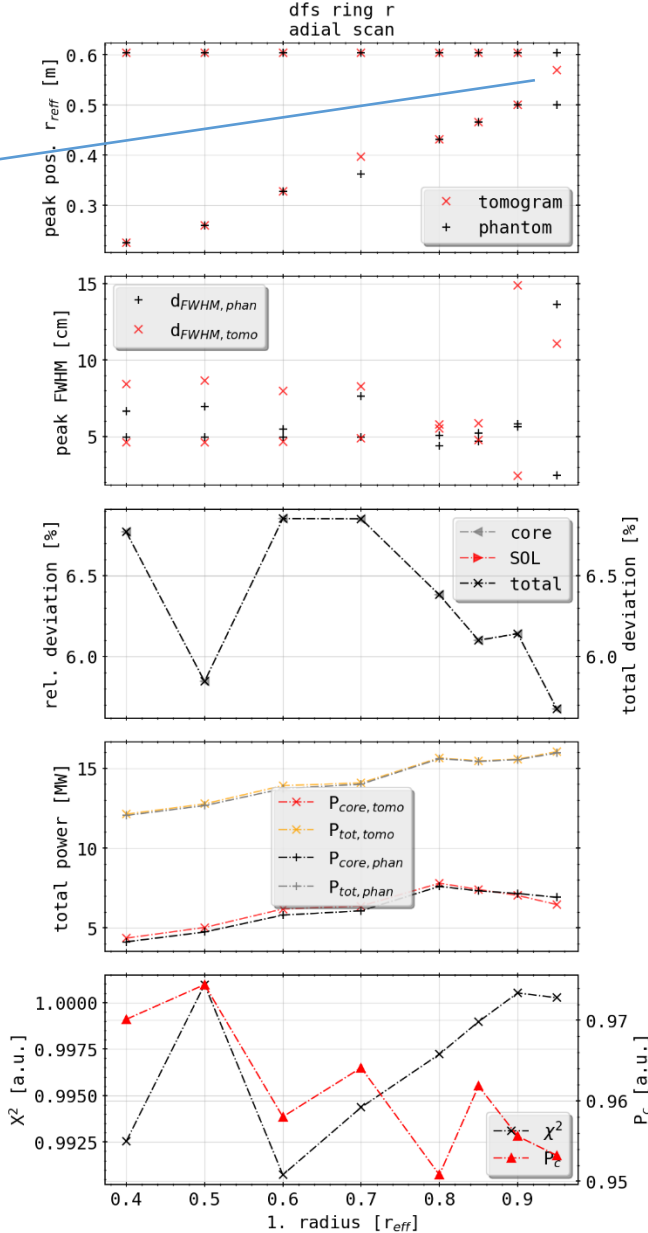
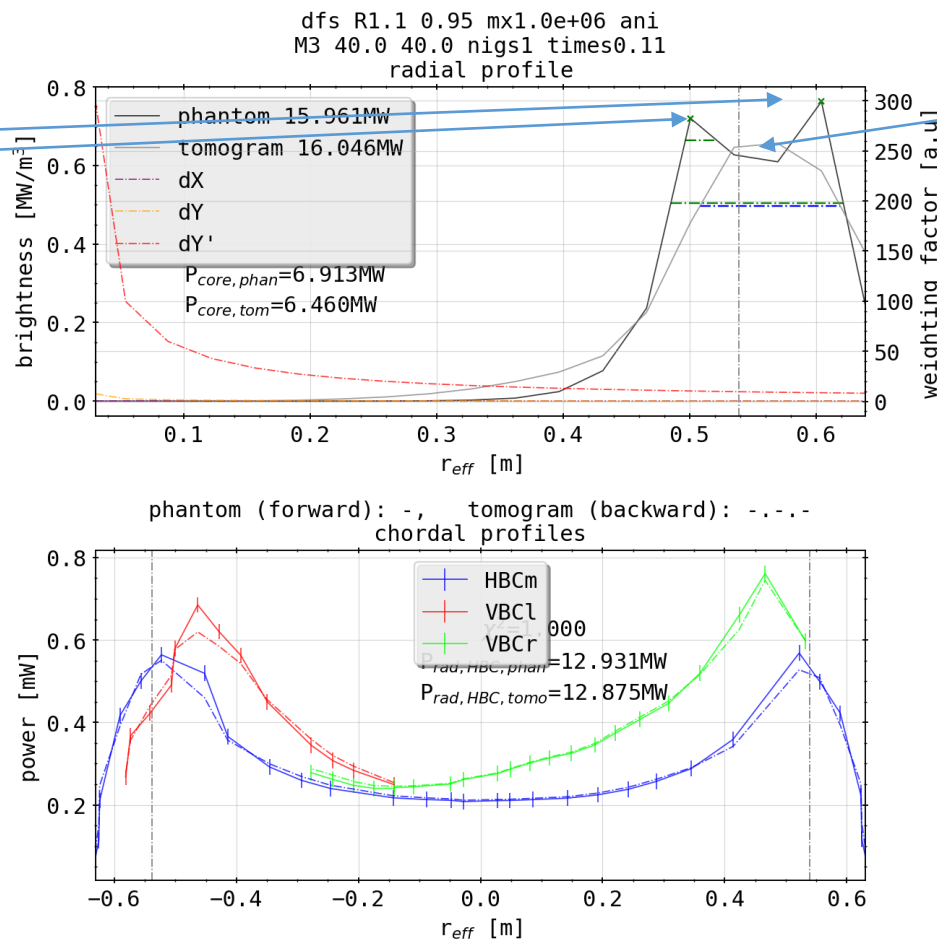
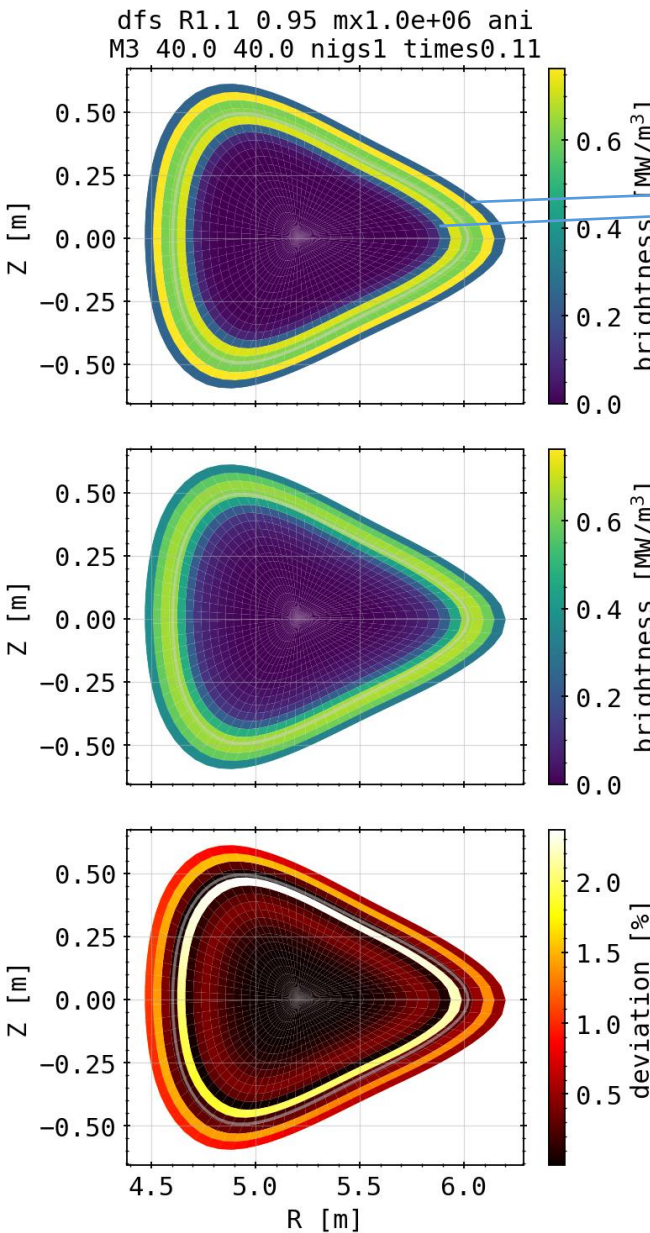
- same chordal profiles with 5% random error, yields same results
- 5% error double of measured

Phantom Test: Double Bright Rings



➤ clear separation of radiation zones,
also radial profile

Phantom Test: Double Bright Rings

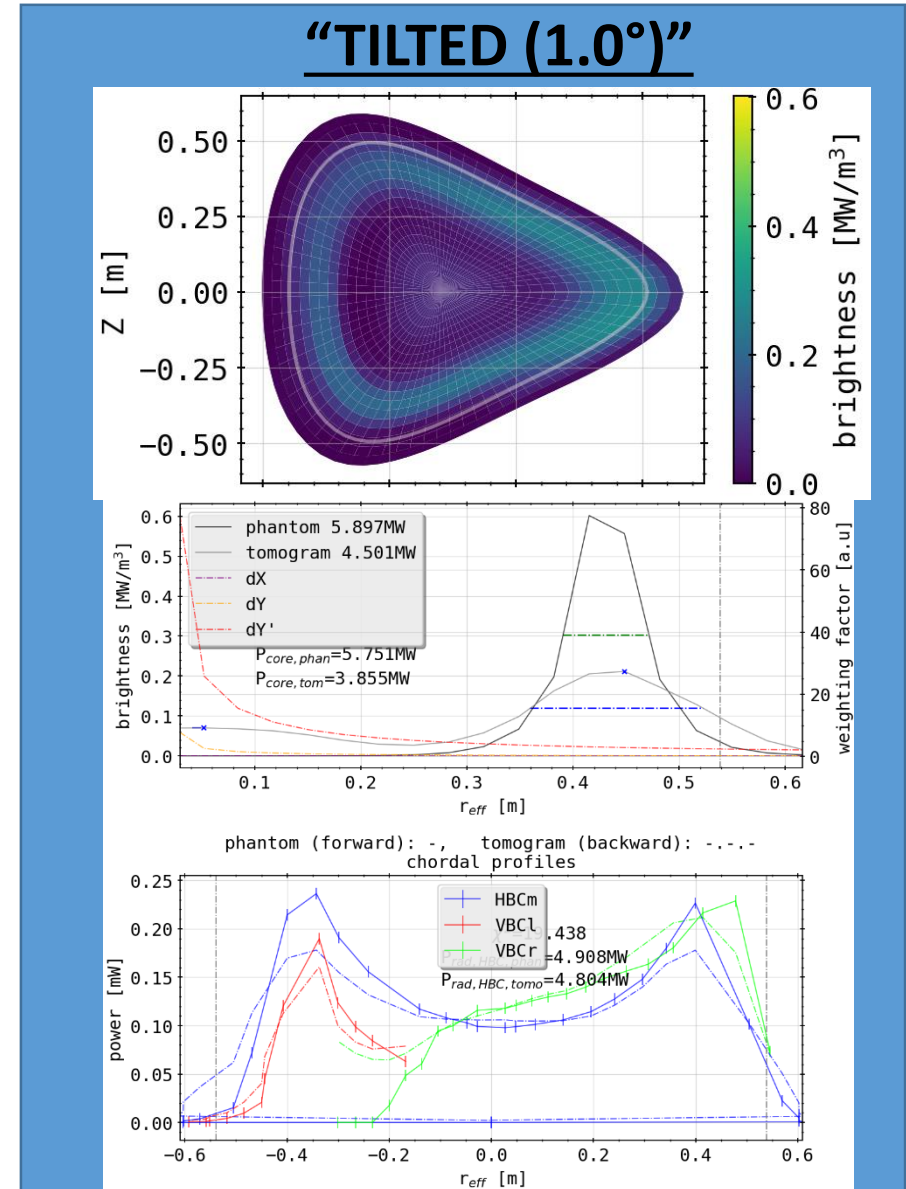
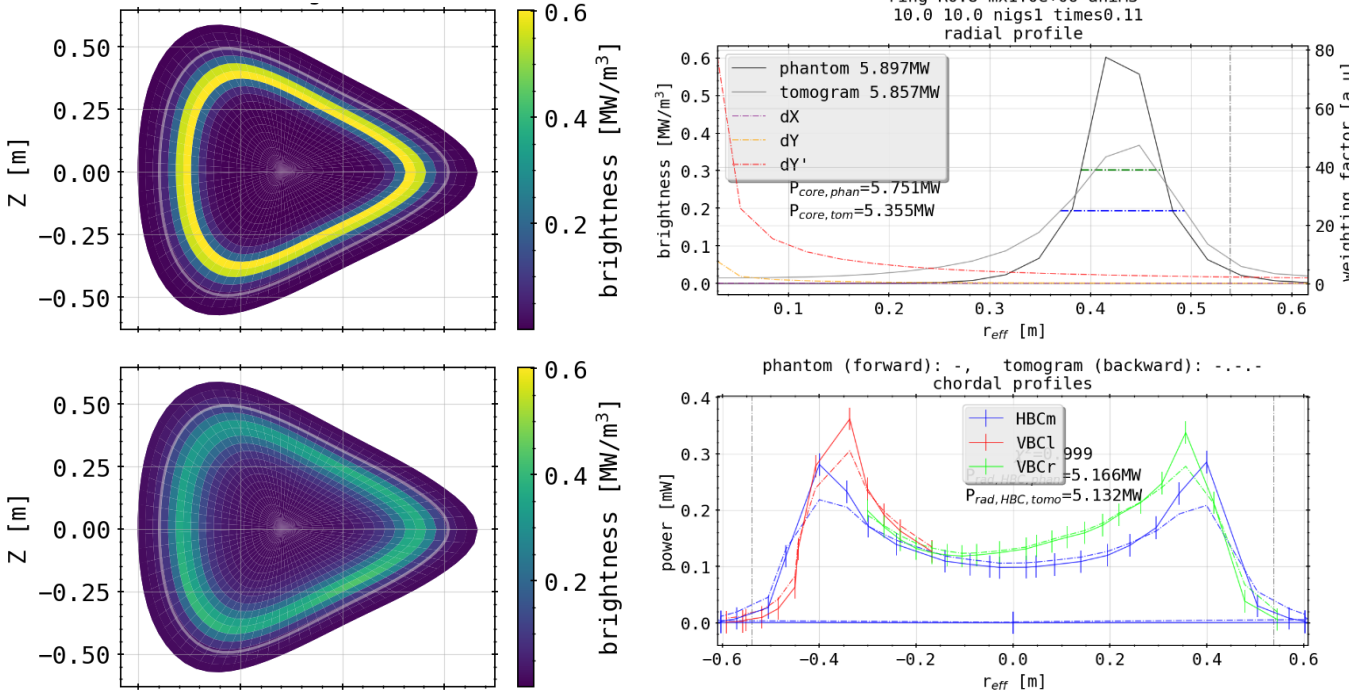


➤ merging of profiles in reconstruction,
minimum resolvable structures
approx. >0.15m in radial direction

Phantom Test: Bright Ring with Intrinsic Error

- Use poloidally rotated camera geometry to calculate forward model and original to do the backward calculations
- assuming error measurement of camera position

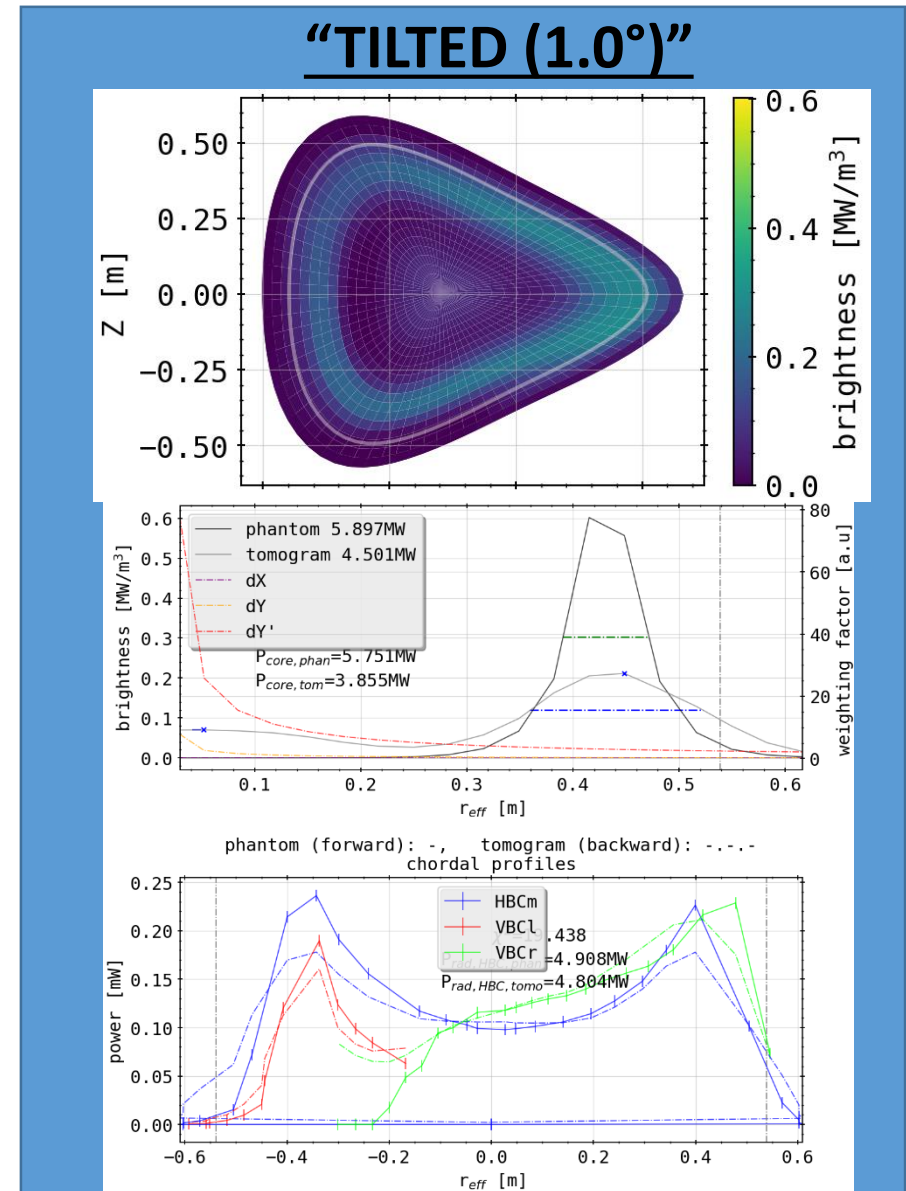
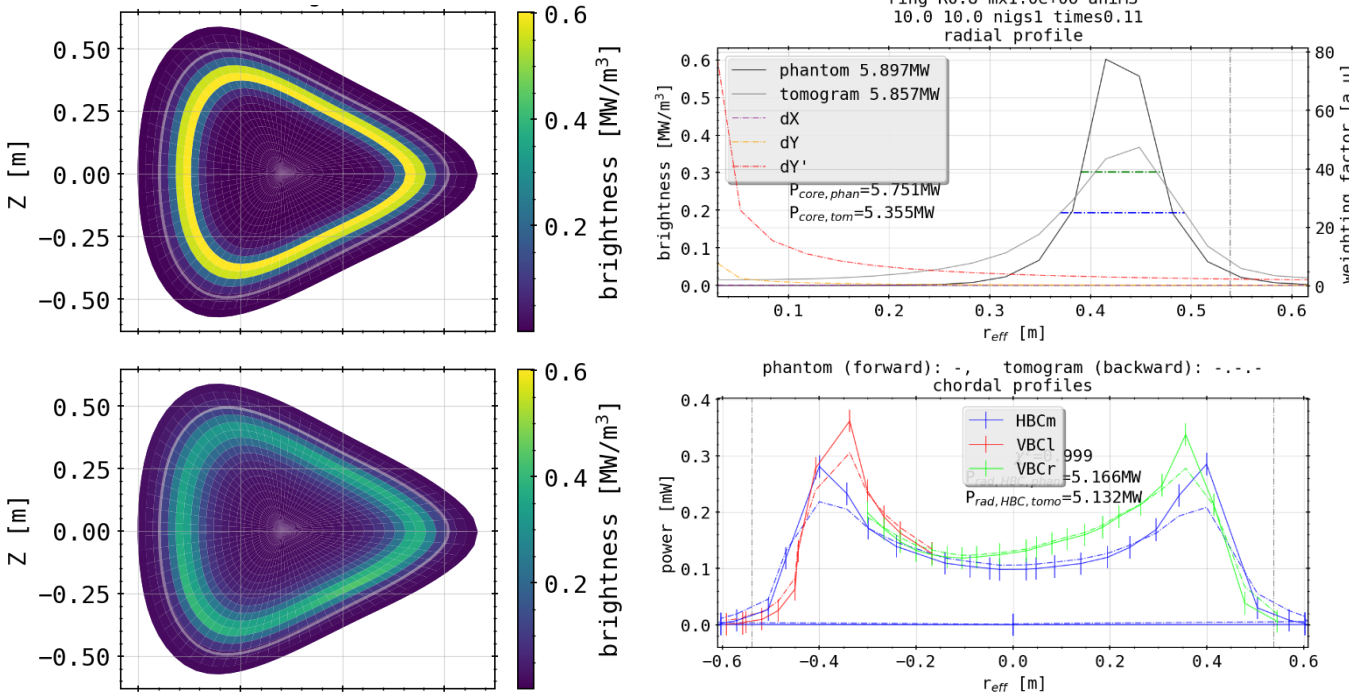
“ORIGINAL”



Phantom Test: Bright Ring with Intrinsic Error

- reconstruction challenged with unmatching forward and backward emissivity geometries
- very large χ^2 indicates conflict in input data, reconstruction however *similar*

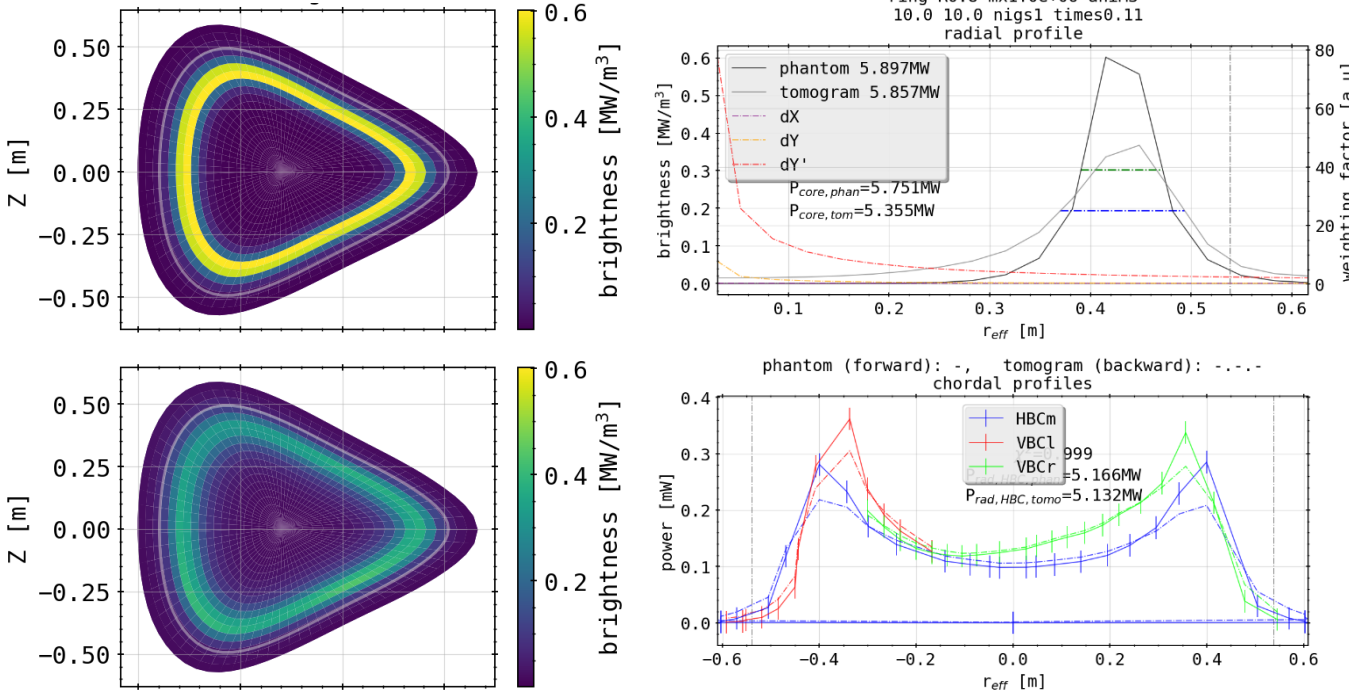
“ORIGINAL”



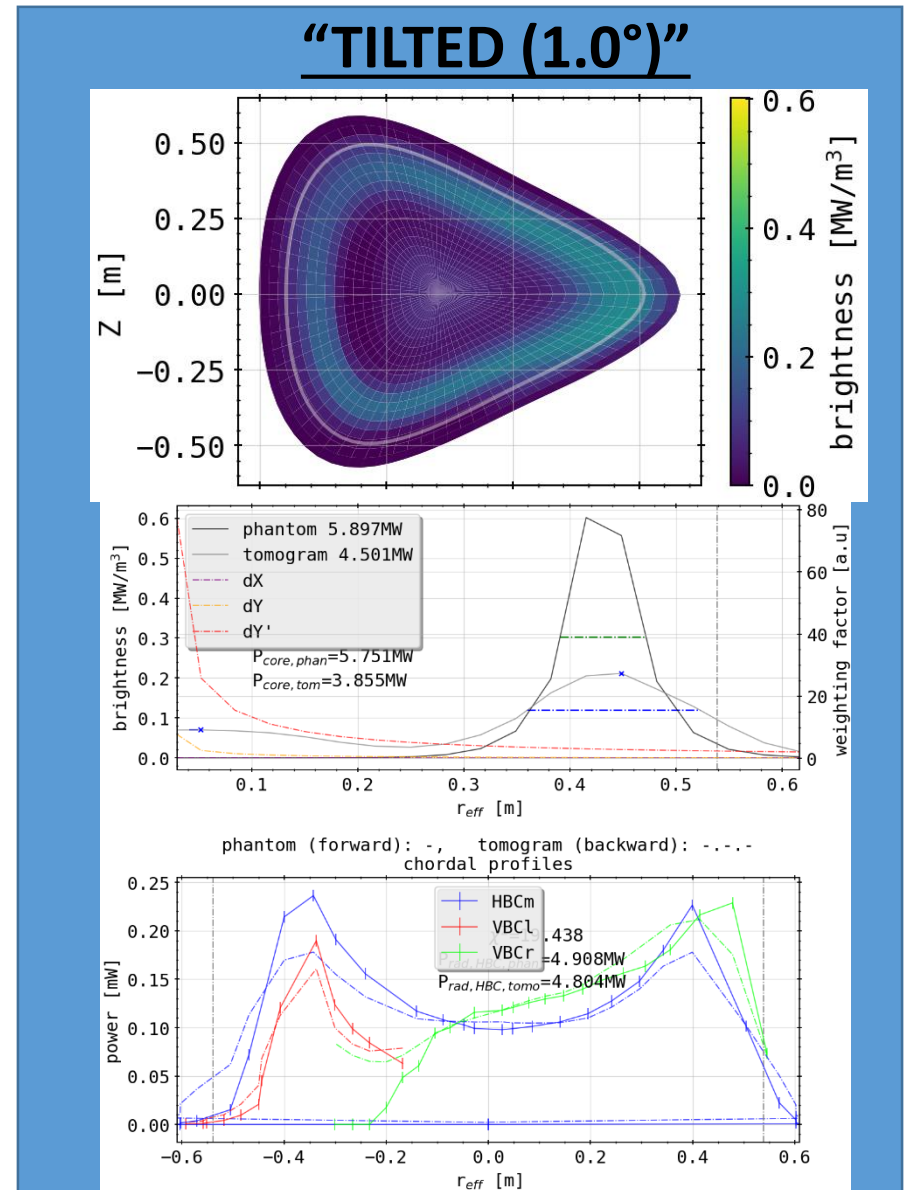
Phantom Test: Bright Ring with Intrinsic Error

- integrated and extrapolated powers diverge from each other as profiles do not fit
- behaviour to be expected if line of sight geometry is disturbed by plasma vessel distortions

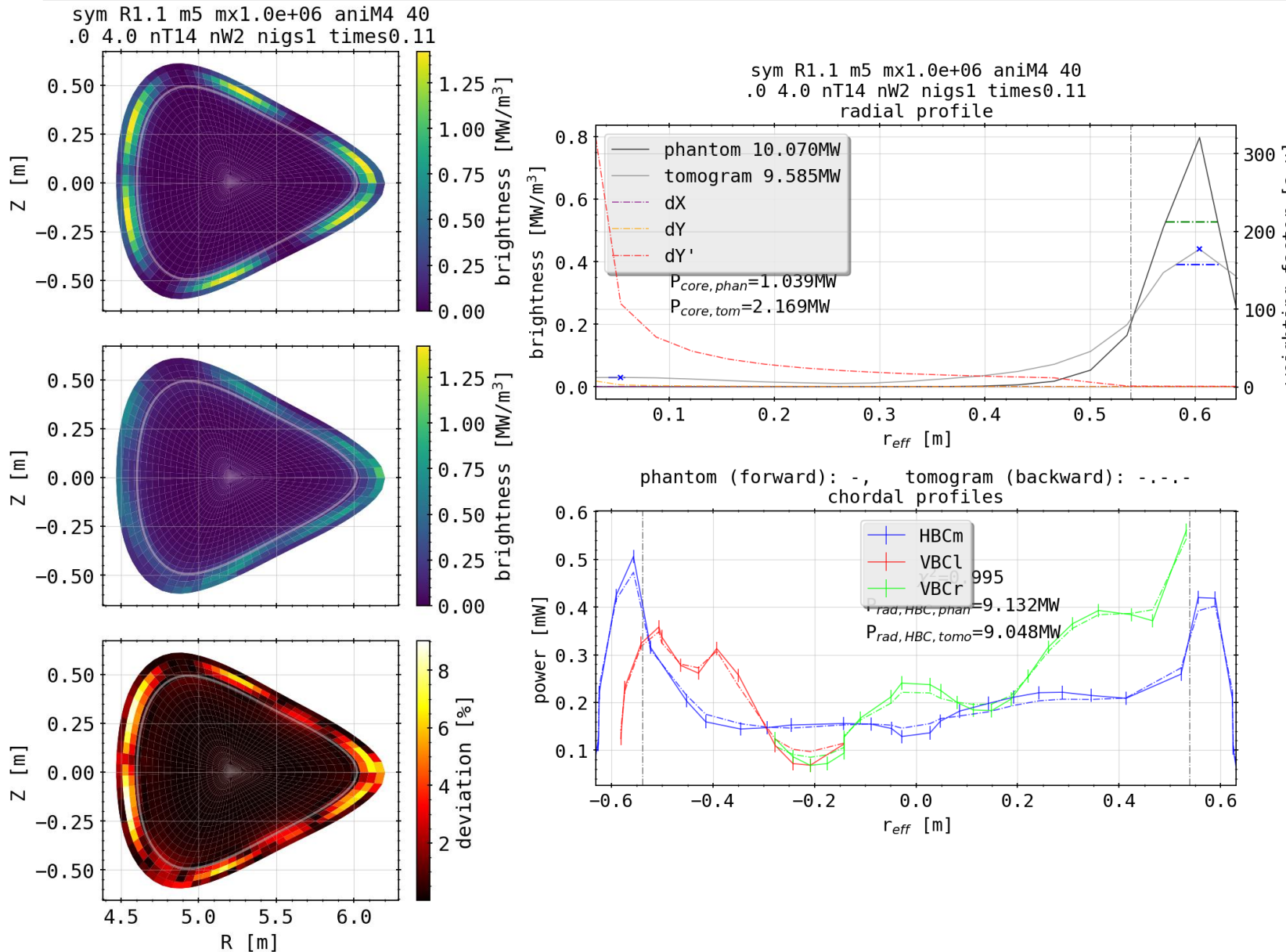
“ORIGINAL”



“TILTED (1.0°)”

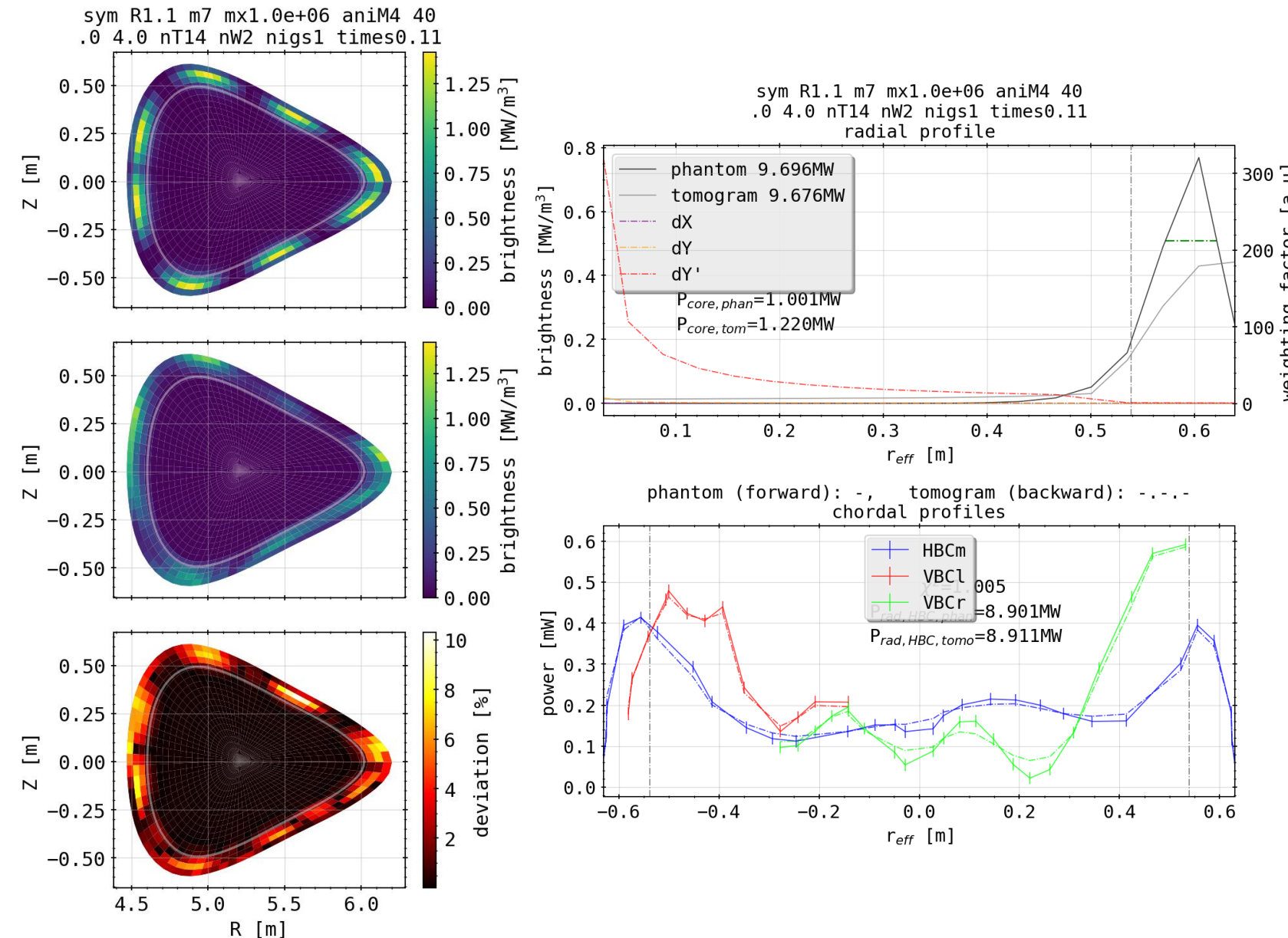


Phantom Test: Symmetric Island Mimic (mode = 5)



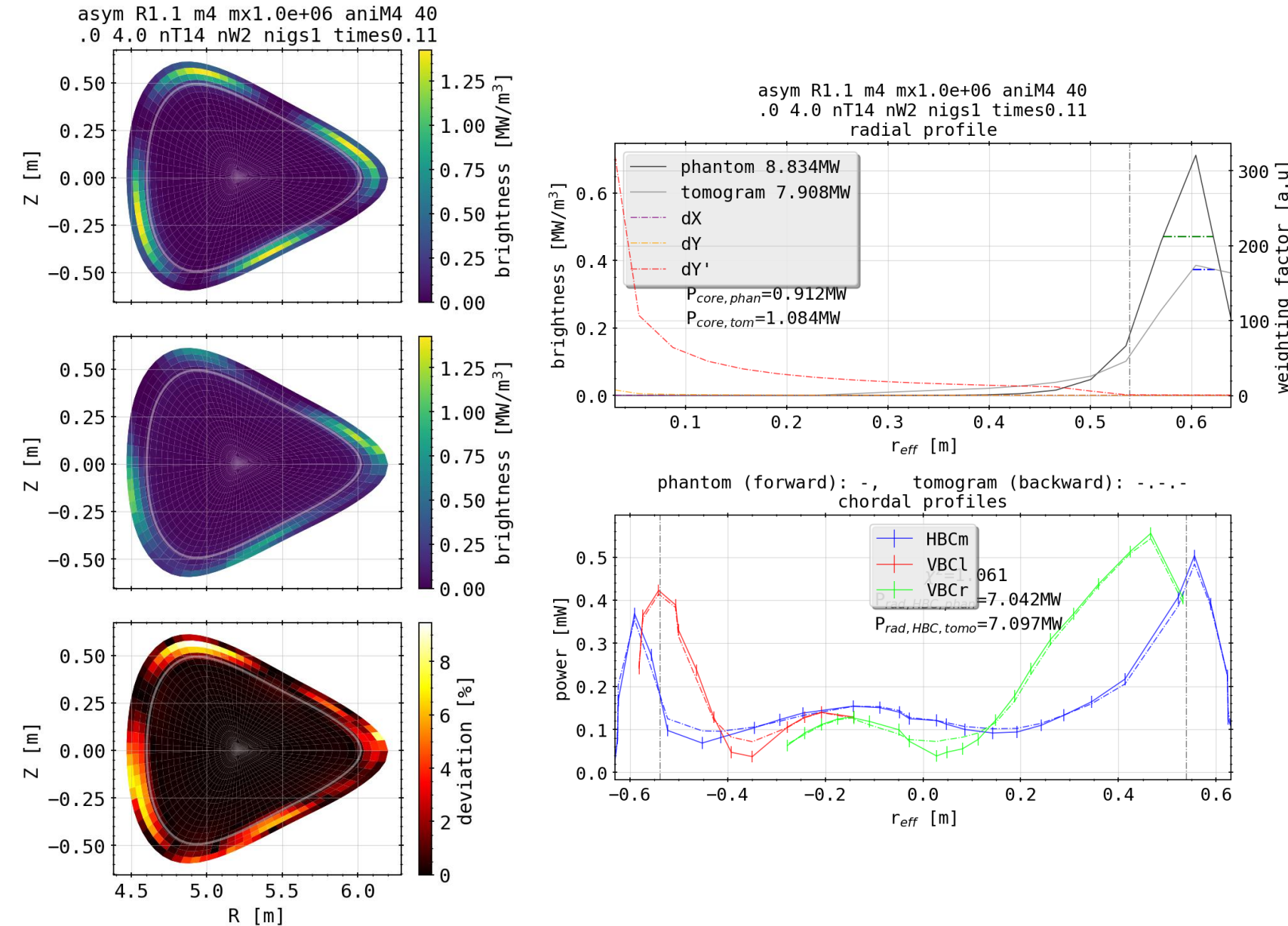
- imitating 5 fold island chain around confinement area
- relatively good match, both radially and poloidally
- redeposition of emissivity at center outboard side where line of sight density is highest
- in contrast: worse resolution of islands on inboard side

Phantom Test: Symmetric Island Mimic (mode = 7)



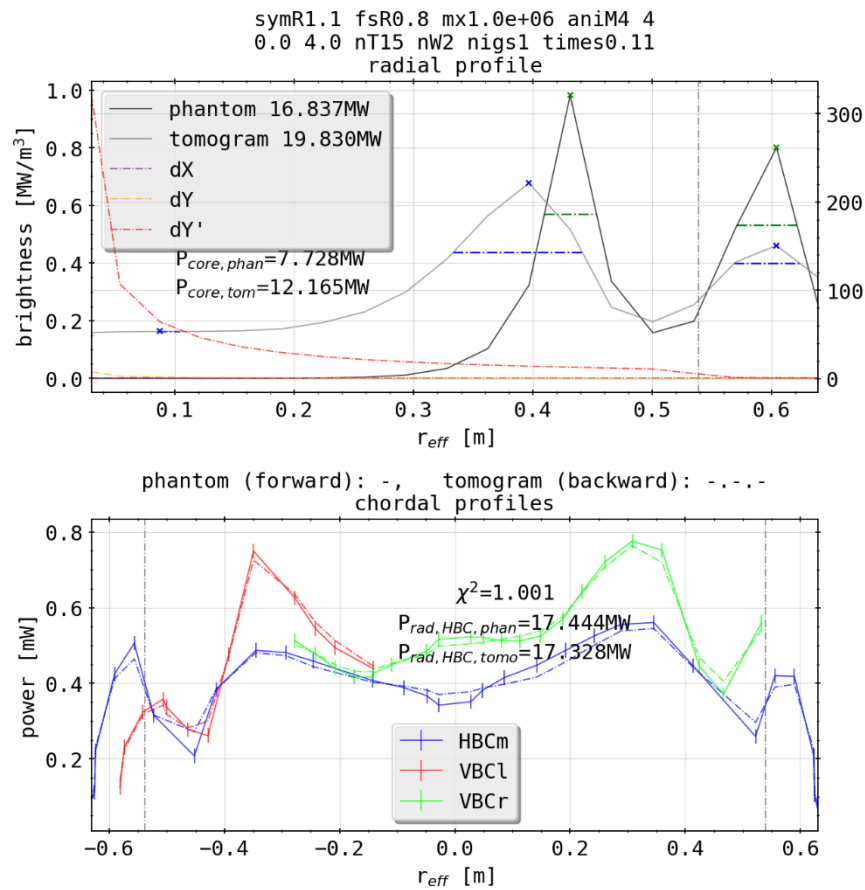
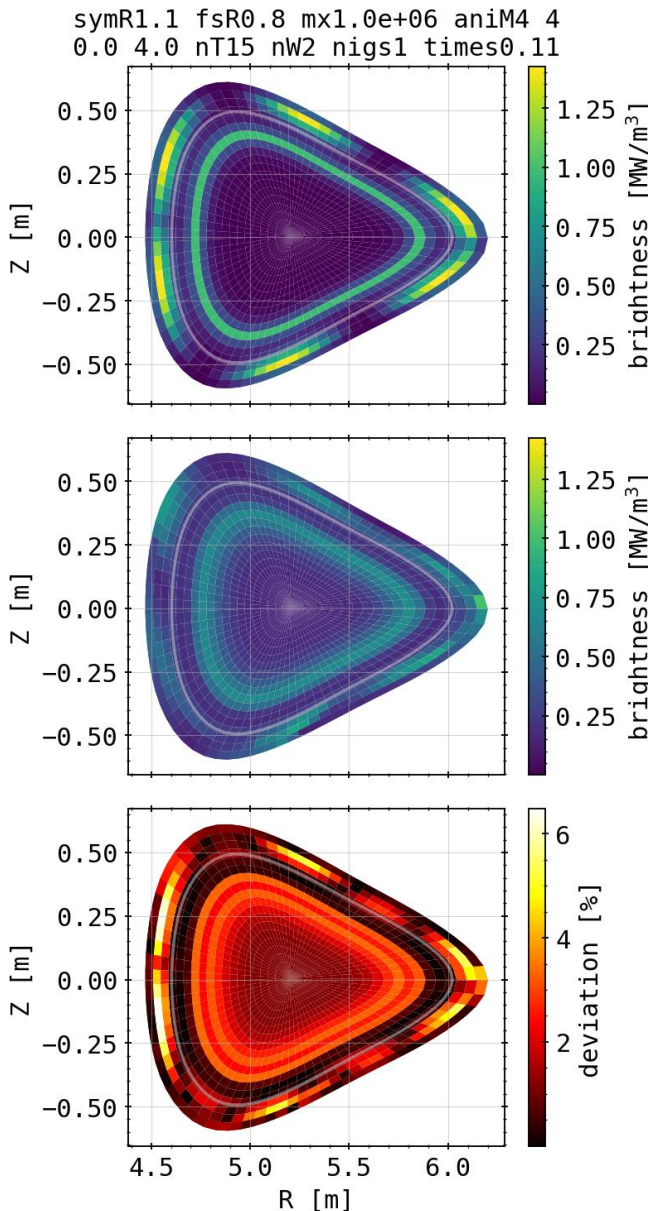
- artificial 7 fold island
- again good match overall
- stronger anisotropy between individual islands in intensity
- depending on number, single spots might be overshadowed by others with respect to the tangential lines of sight from HBC/VBC

Phantom Test: Asymmetric Island Mimic (mode = 4)



- artificial 4 fold islands sinusoidally distributed around core
- match as before, profile reconstruction easily readable
- overshadowing from outboard *island* represents issue with line integration along the SOL from both camera arrays

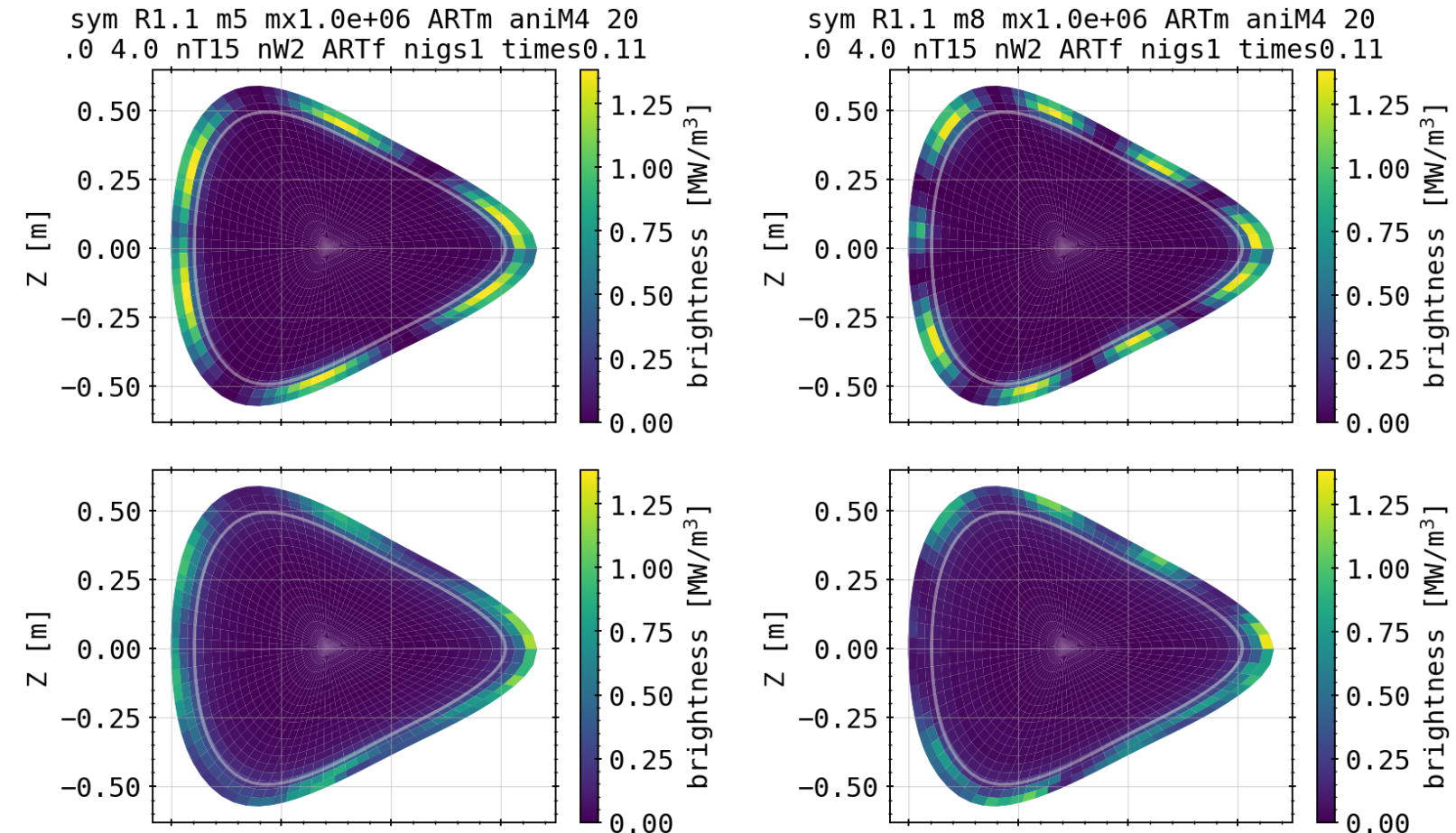
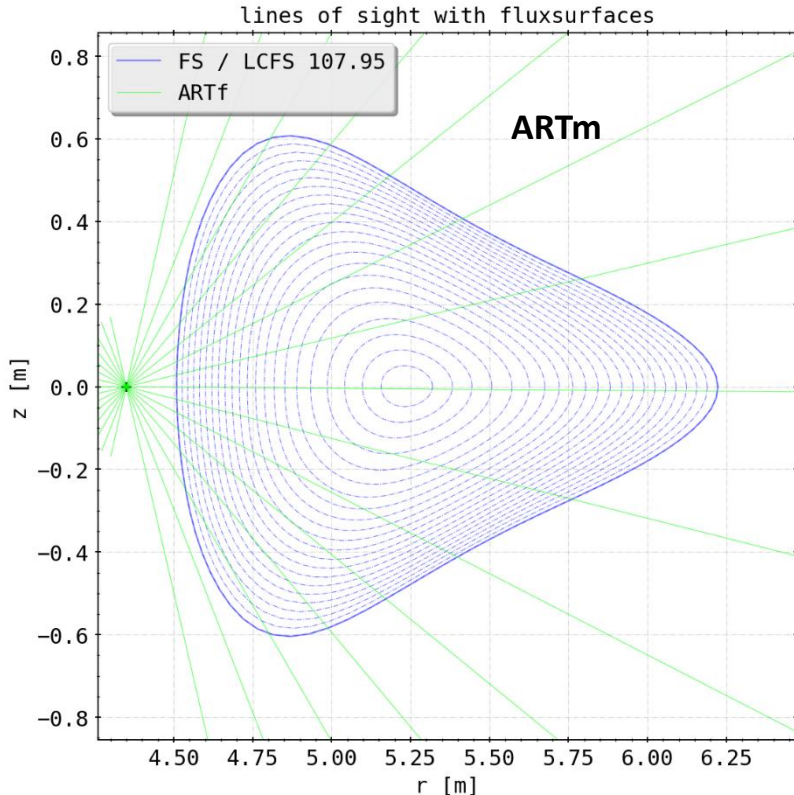
Phantom Test: Island Mimic and Core Radiation



- additional profile on the inside of the island mimic does not deteriorate the quality of the spot reconstruction
- 2D integrated power diverges, however P_rad from chordal profiles is in agreement
- smearing effect observed before creates issues when multiple surrogate structures meet

Phantom Test: New Cameras Towards Island Mimic

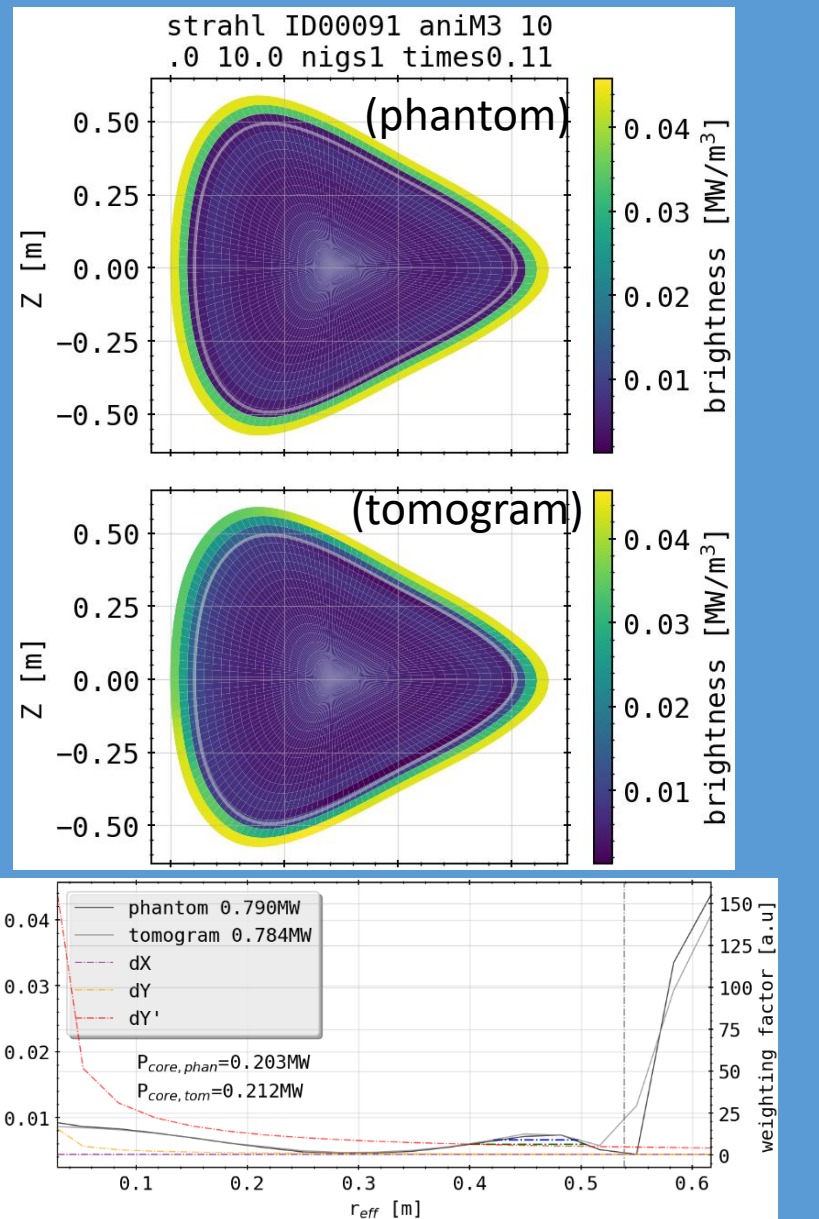
- adding camera, 15 channels



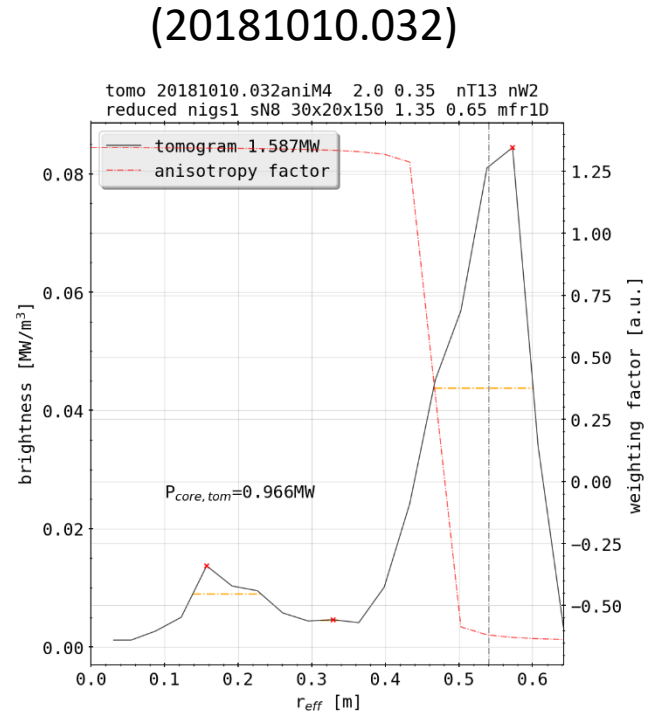
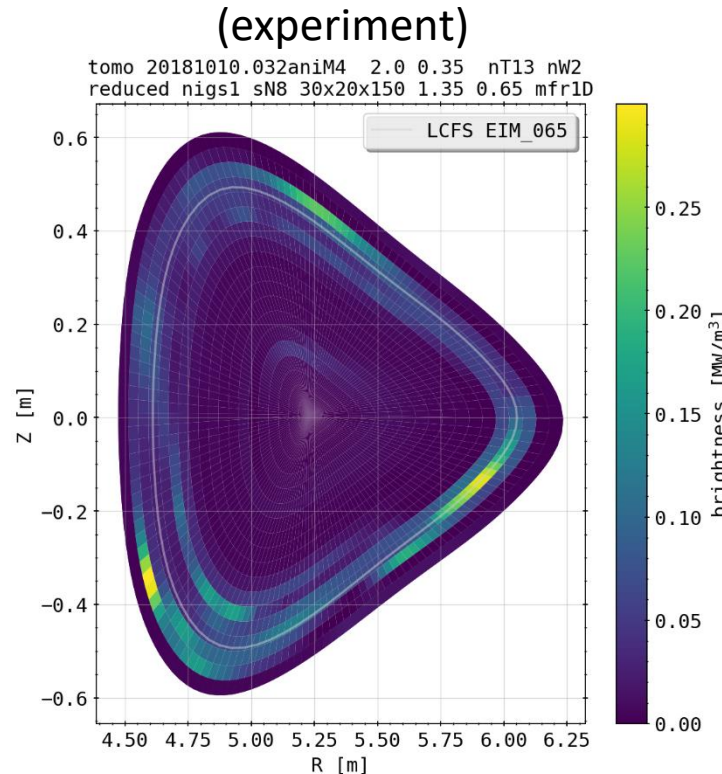
- better island positioning and relative intensity, symmetry increased overall
- overshadowing persistent from HBC perspective

STRAHL and XP: 20181010.032 Comparison

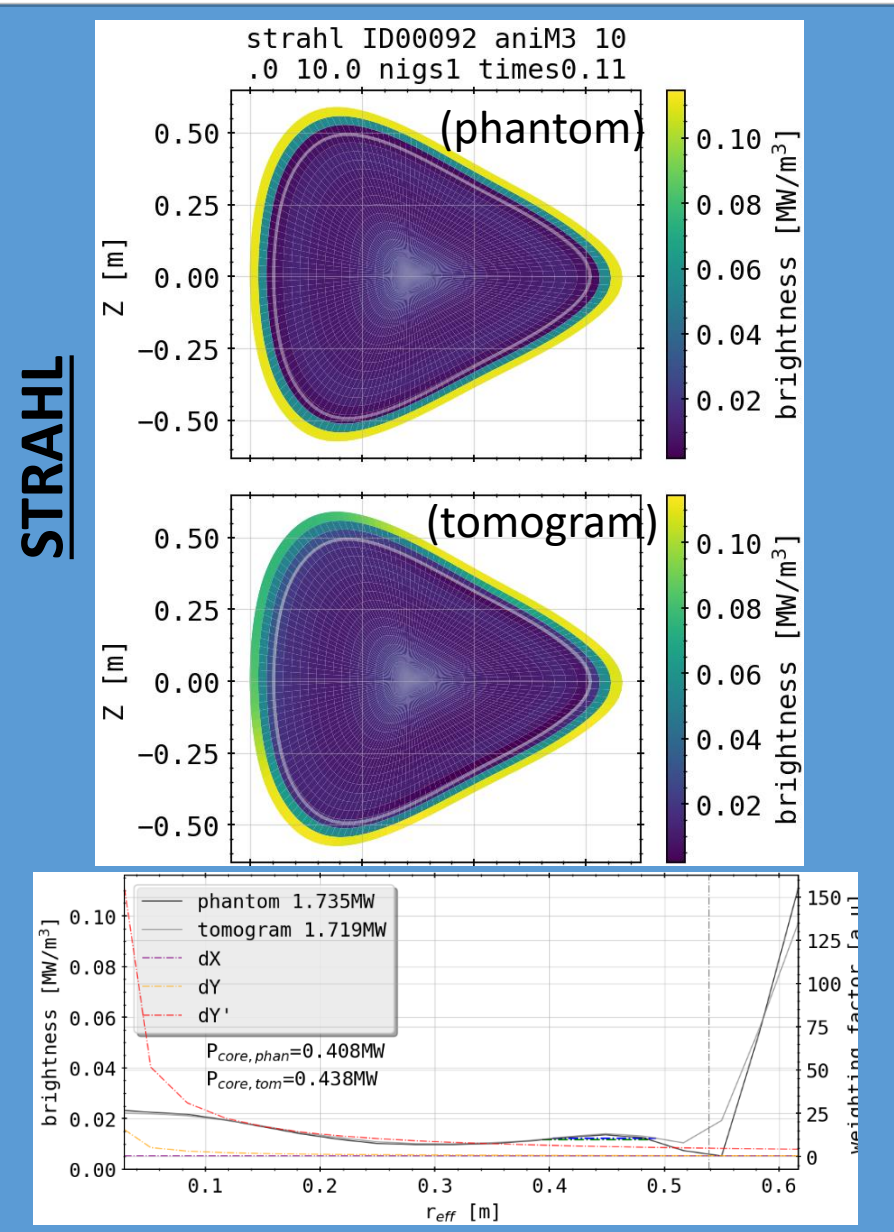
STRAHL



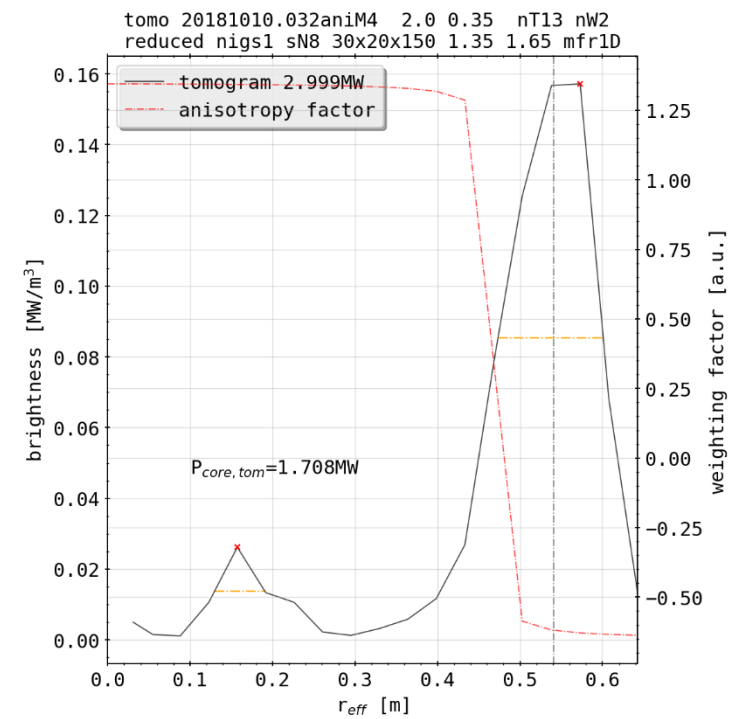
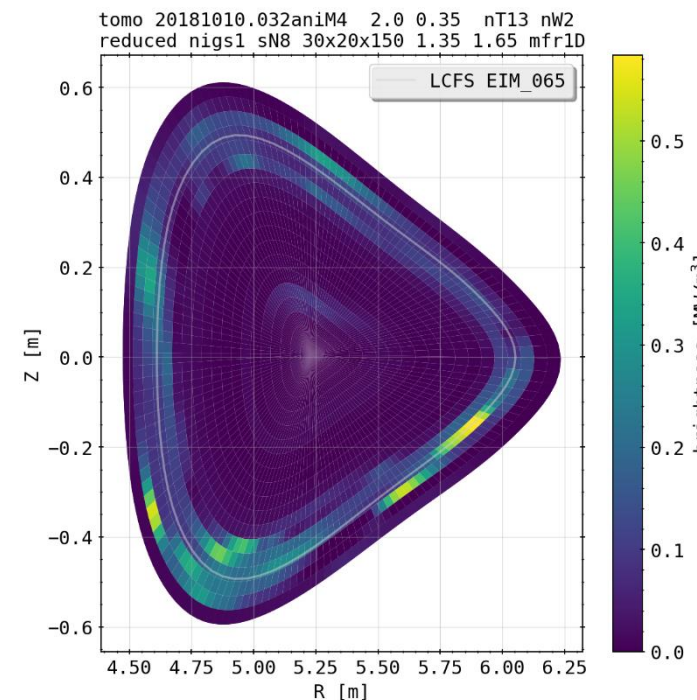
radiation fraction = 33%



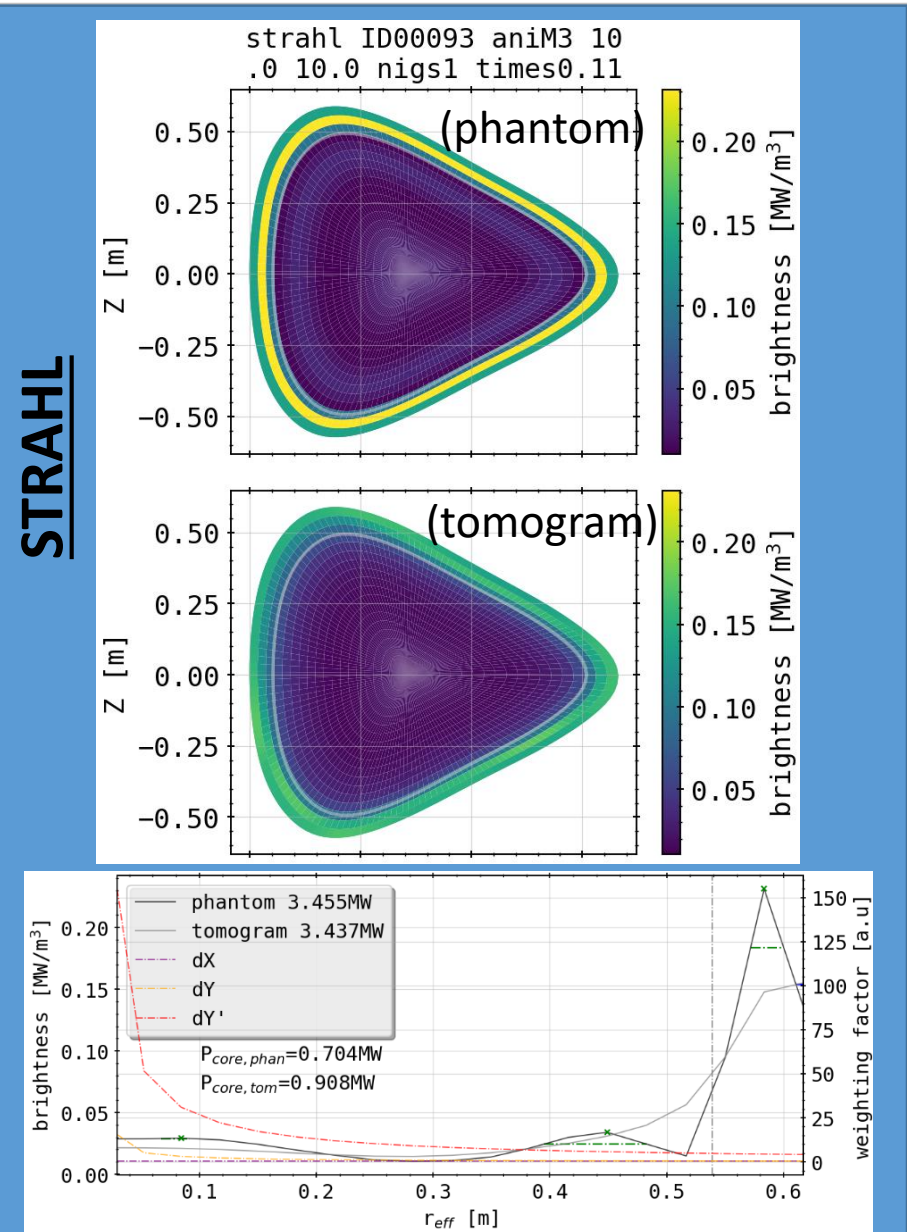
STRAHL and XP: 20181010.032 Comparison



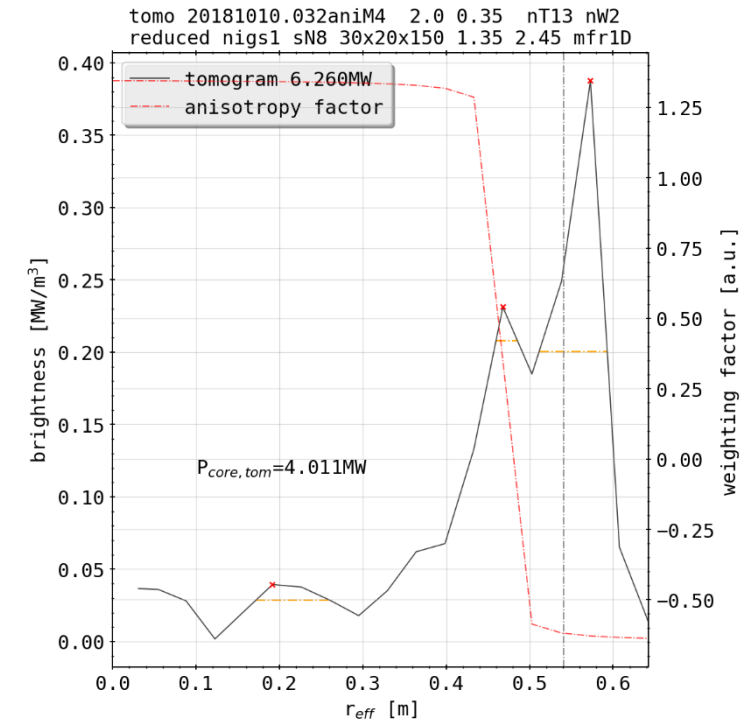
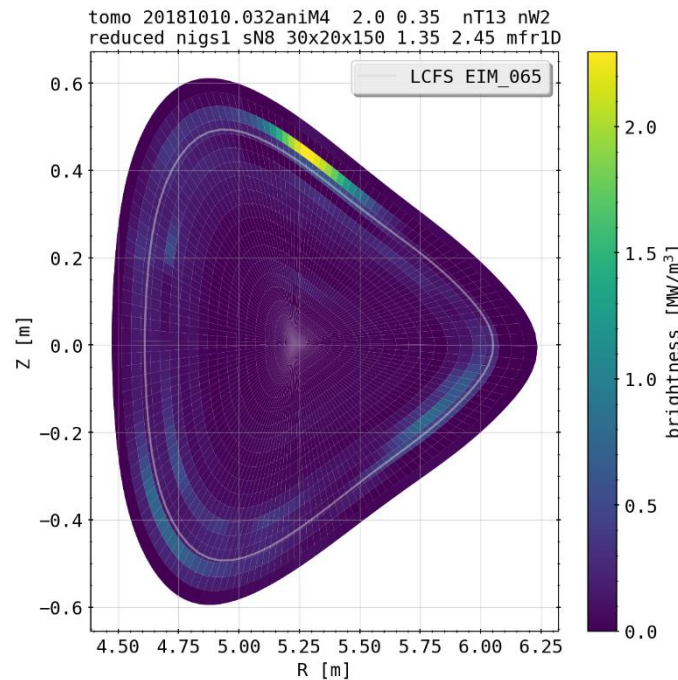
radiation fraction = 66%



STRAHL and XP: 20181010.032 Comparison

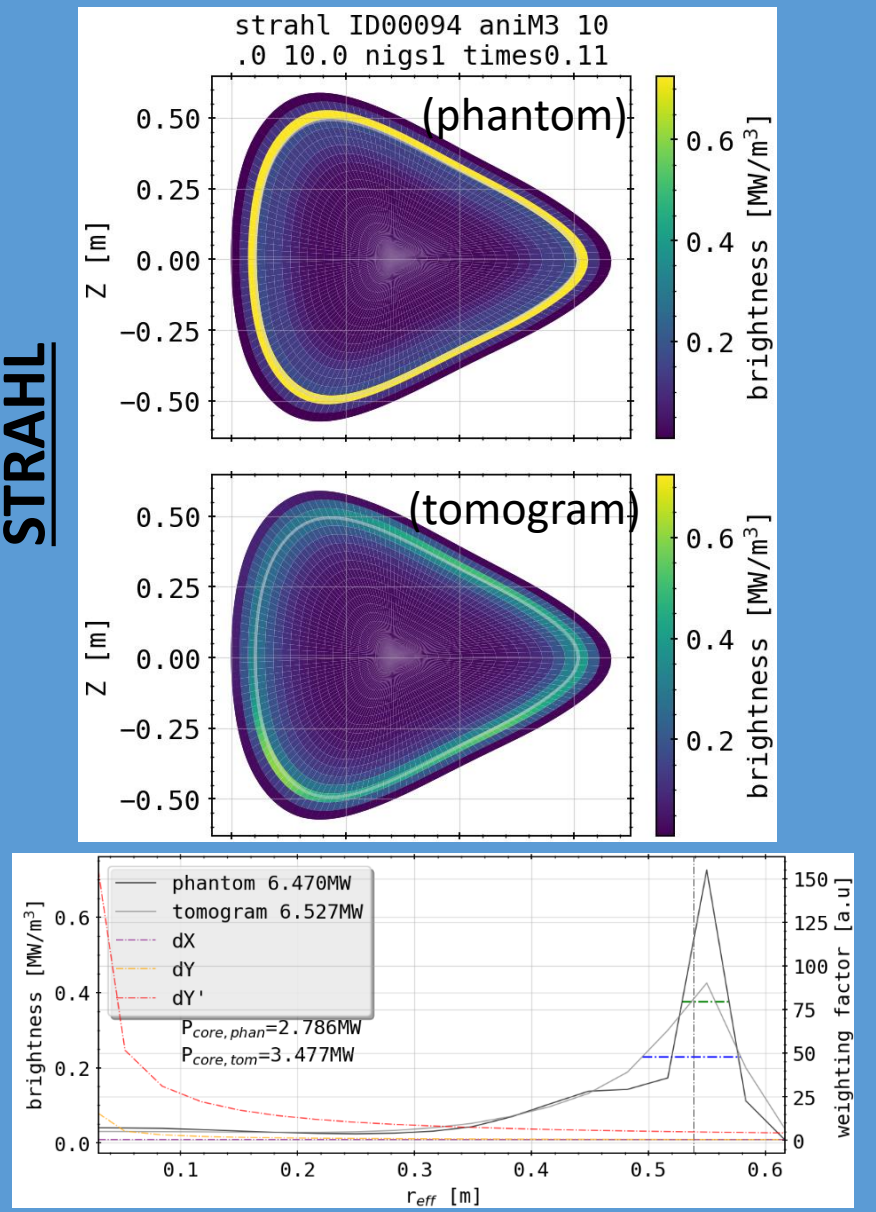


radiation fraction = 90%

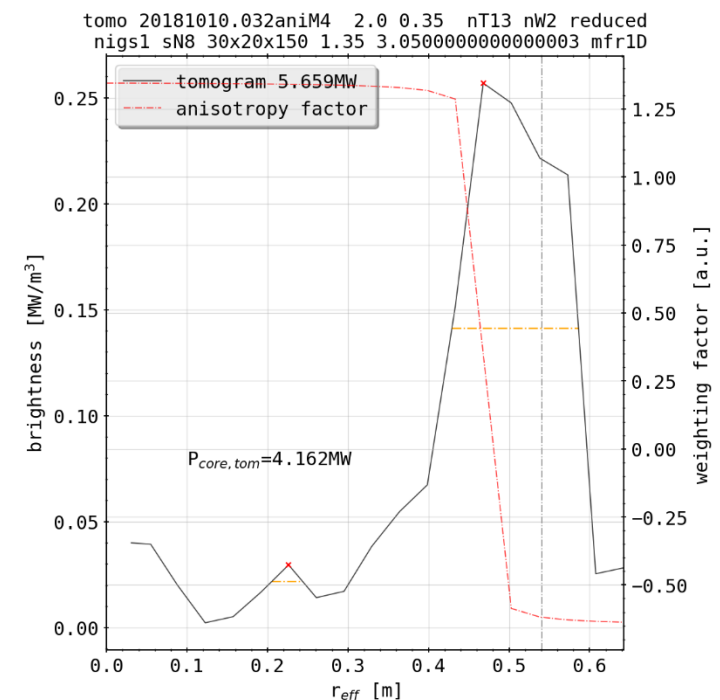
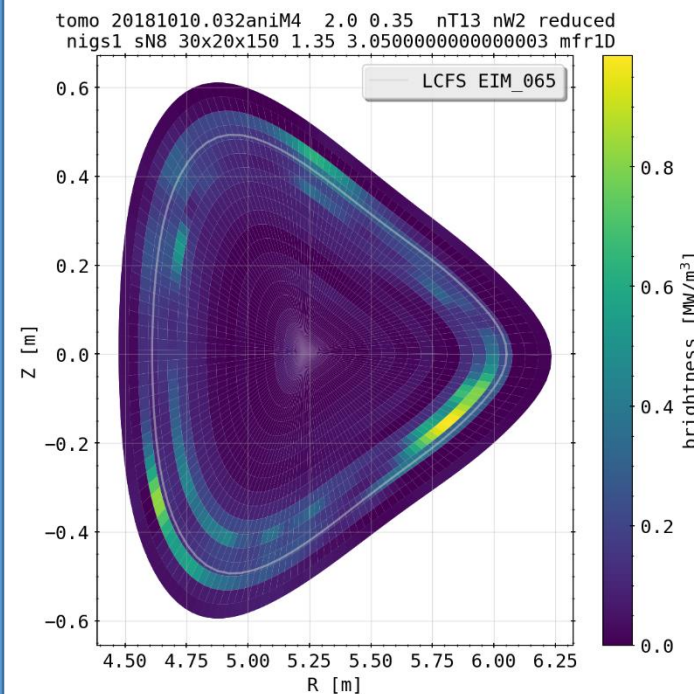


STRAHL and XP: 20181010.032 Comparison

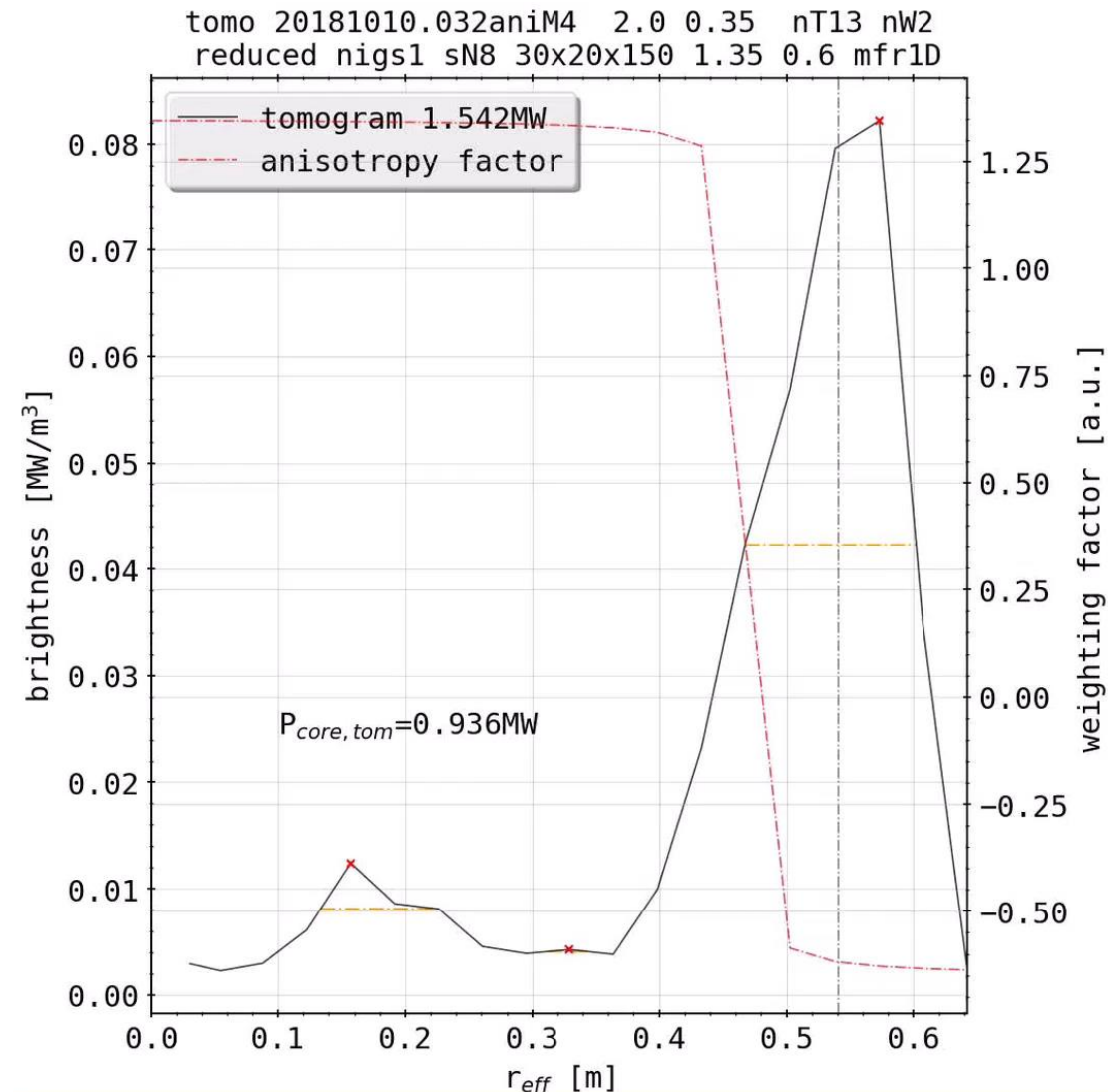
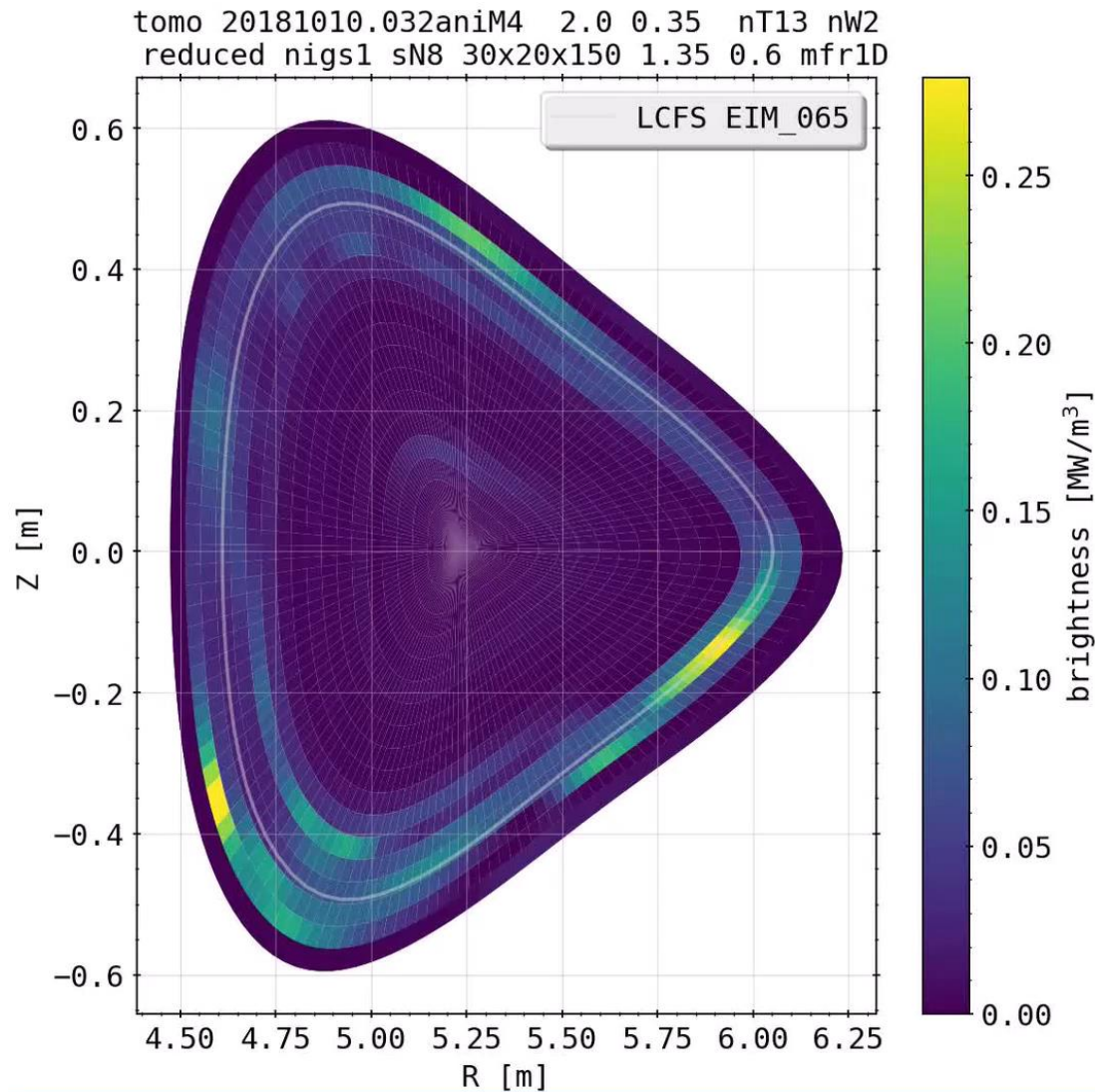
STRAHL



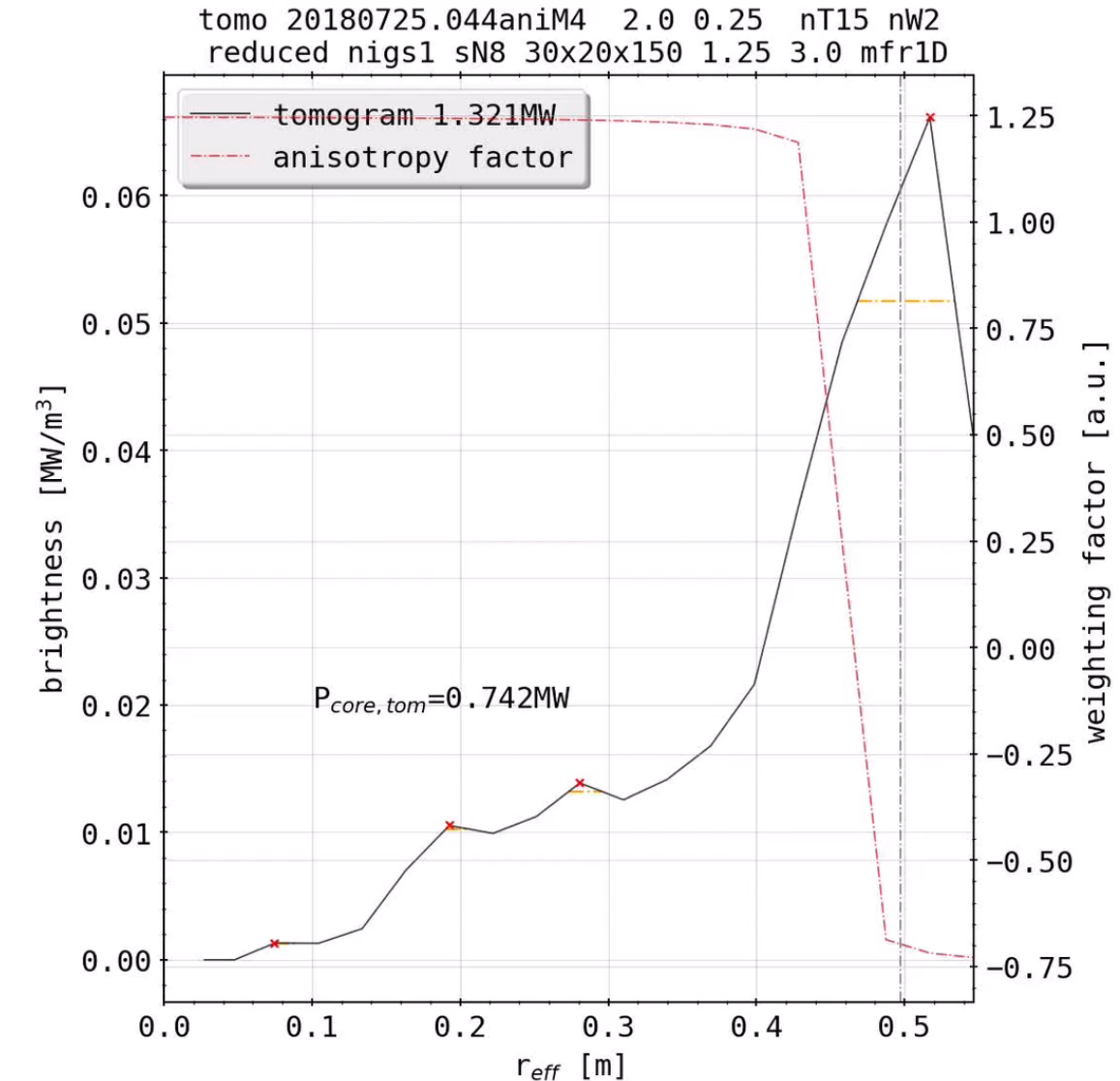
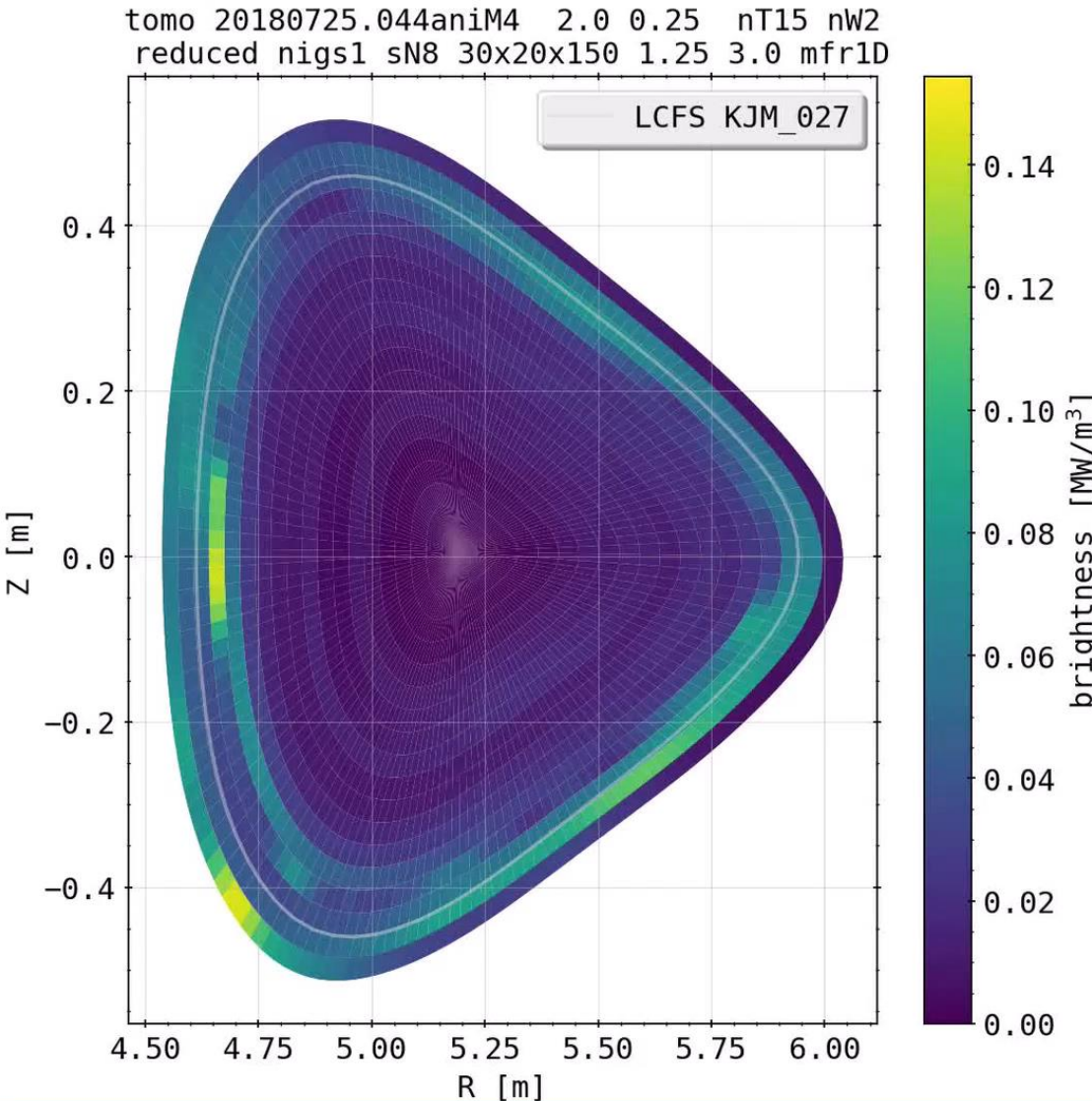
radiation fraction = 33%



XP: 20181010.032



XP: 20180725.022



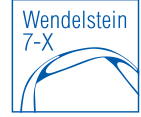
Preliminary Conclusion and Outlook



- likely good (best?) resolution of inversion domain, both with reasonable accuracy and calculation time is 20x75 cells (radial times poloidal)

- additional radial or poloidal points only add time to calculation and possible free parameters to fit emissivity (avoidable by changing the gradients along the aforementioned dimensions accordingly)

Preliminary Conclusion and Outlook



- considering a given emissivity profile shape, there exists an ideal set of K factors constraining the ratio of poloidal and radial gradients according to the χ^2 optimisation
- not necessarily the same as defined by the lowest 2D deviation, whose optimisation also yields an optimal set of K factors
- radial positioning of profiles is subject to the selection of K factors over the radius

Preliminary Conclusion and Outlook



- poloidally distributed profiles are, so far the data set suggests, the hardest to reconstruct properly (especially on the inboard side)
- asymmetric characteristics can be property of the underlying emissivity profile to the tomography, however some are introduced due to the line of sight geometry
- combinations of profile shapes, especially poloidally symmetric and any else become hard to distinguish from one another (see ring and island mimic)

Preliminary Conclusion and Outlook

- bright spots on-/off-axis and, e.g. bright rings can be separated from each other depending on the distance
- individual bright sheaths can no longer be reconstructed radially when closer than 0.2m
- reconstructions of forward calculated STRAHL simulations are largely accurate in position and value
- reference XP 20181010.032 difficult to reconstruct, subject to difference in forward and backward model?

Preliminary Conclusion and Outlook



- possibly find better approach to K factor profile shape for island mimics or combinations (double rings as well?) and asymmetric phantoms

- check orders of magnitude/units of results for plausibility

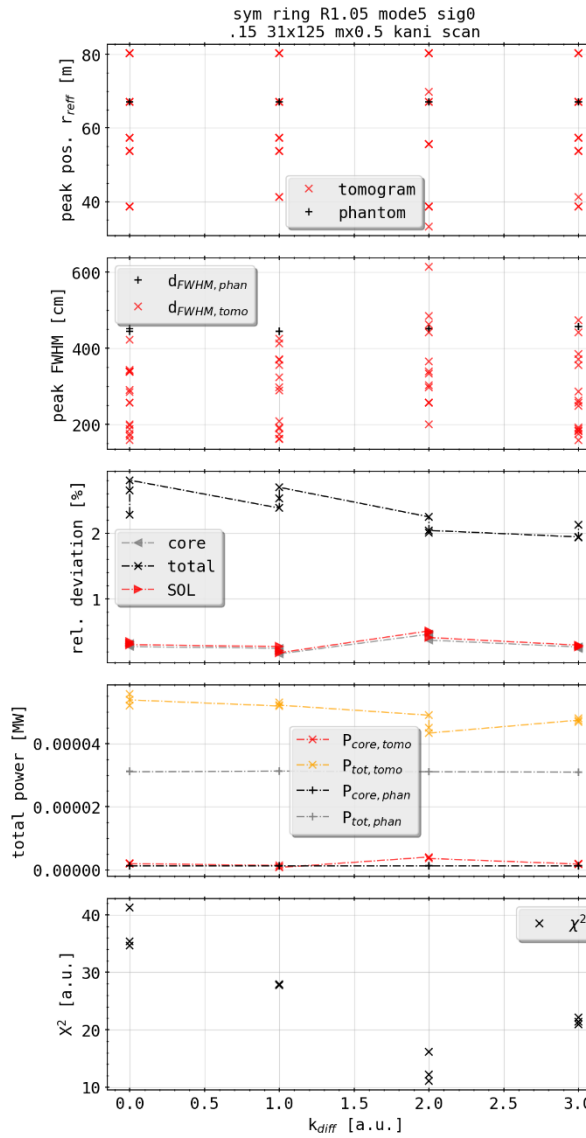
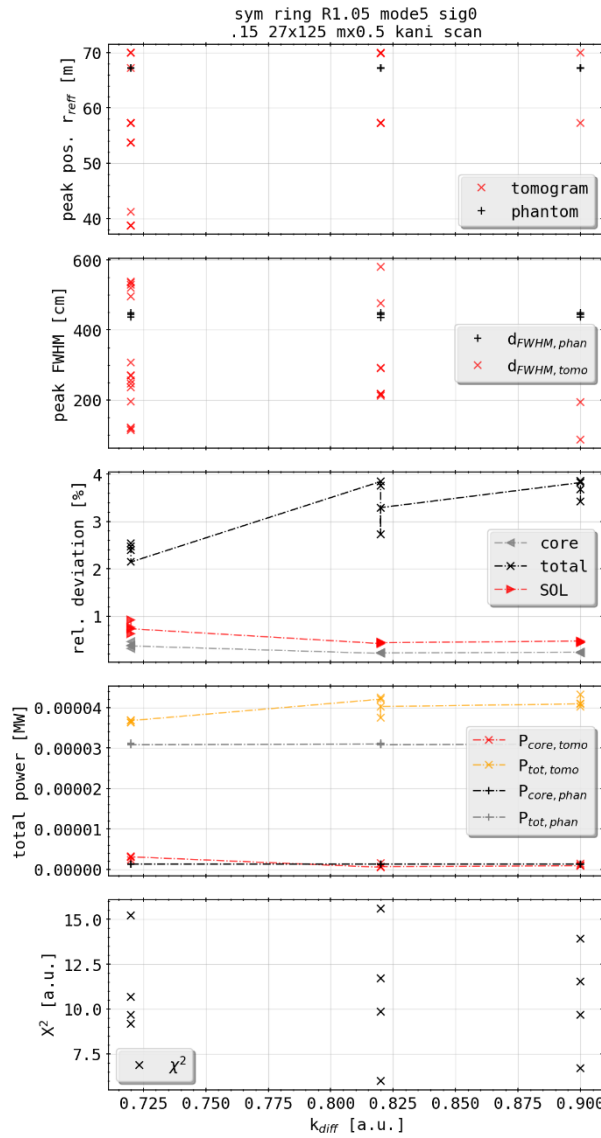
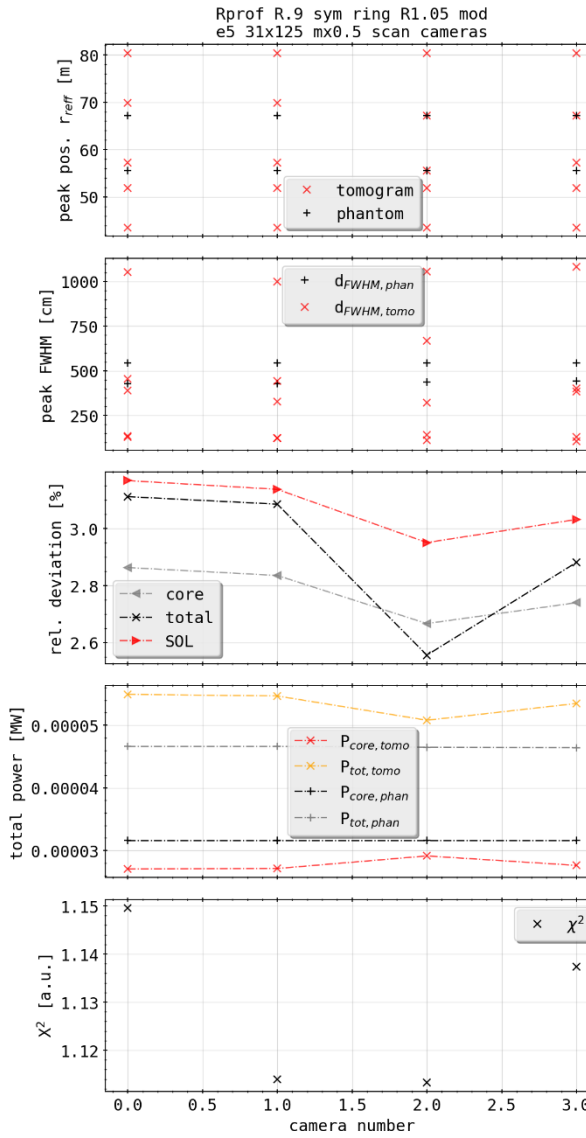
Completed or Closed

- correlation analysis for channel selection
- find best channel/selection or combination of channels from any camera to suit the total radiated power loss the best (limited to one-three single experiments/discharges)
- interpretation in tandem with improved Thomson scattering profiles from Minerva and impurity content radiation/oxygen
- analyse localisation of impurity seeding and hence radiation position/sensitivity of QSB; transport comparison/analysis with STRAHL
- TOMOGRAPHY
- implementation of findings from channel correlation to inversion, see whether the amount or channel distribution/geometry is efficient

Uncompleted or Not Started

- thermal gas beam feedback is arranged on n_e , not P_{rad} in those two discharges
→ $n_e + \Delta n_e \Rightarrow P_{rad} + \Delta P_{rad}$, need to look at $\Delta N H_2$?
- finish RSI paper scrap with images, graphs, references
- comparison between different methods, e.g Minerva/minimum Fischer regularization etc.
- investigate on the different impact of extrinsic impurity seedings from thermal gas beam injection (QSQ)
- set up database to maybe find common/individual scaling laws in tandem with relation to n_e , W_{dia} , P_{ECRH} etc.

Scans from 2D Results



Scans from 2D Results

